

USARTL-TR-78-9

LEVEL

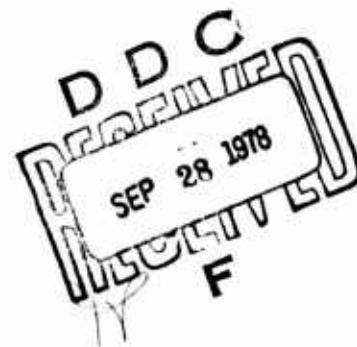


2
@

**EFFECT OF OPERATIONAL ENVELOPE LIMITS
ON TEETERING ROTOR FLAPPING**

AD A0 59 187

L. W. Dooley, S. W. Ferguson, III
Bell Helicopter Textron
P. O. Box 482
Fort Worth, Tex. 76101



July 1978

Final Report for Period June 1976 - August 1977

D D C FILE COPY

Approved for public release;
distribution unlimited.

Prepared for
APPLIED TECHNOLOGY LABORATORY
U. S. ARMY RESEARCH AND TECHNOLOGY LABORATORIES (AVRADCOM)
Fort Eustis, Va. 23604

78 09 26 003

APPLIED TECHNOLOGY LABORATORY POSITION STATEMENT

This report investigates the effect of AH-1G/R operational envelope limits on flapping and examines several methods of extending the recommended operational envelope through reduced flapping or increased safety margin. The hybrid computer version of C81 used for the flapping prediction simulations did not, however, include the aeroelastic rotor blade feature potentially significant for blade tip deflection prediction. Results of this contract are being combined with results from previous efforts to identify critical teetering rotor helicopter flight conditions and maneuvers, and to recommend the most promising method of extending operational envelopes by alleviating the consequences of high flapping. The results of this effort, while not exhaustive, are believed to be technically sound and within the originally intended scope.

Mr. G. Thomas White of the Technology Applications Division served as project engineer for this investigation.

DISCLAIMERS

The findings in this report are not to be construed as an official Department of the Army position unless so designated by other authorized documents.

When Government drawings, specifications, or other data are used for any purpose other than in connection with a definitely related Government procurement operation, the United States Government thereby incurs no responsibility nor any obligation whatsoever; and the fact that the Government may have formulated, furnished, or in any way supplied the said drawings, specifications, or other data is not to be regarded by implication or otherwise as in any manner licensing the holder or any other person or corporation, or conveying any rights or permission, to manufacture, use, or sell any patented invention that may in any way be related thereto.

Trade names cited in this report do not constitute an official endorsement or approval of the use of such commercial hardware or software.

DISPOSITION INSTRUCTIONS

Destroy this report when no longer needed. Do not return it to the originator.

UNCLASSIFIED

SECURITY CLASSIFICATION OF THIS PAGE (When Data Entered)

19 REPORT DOCUMENTATION PAGE		READ INSTRUCTIONS BEFORE COMPLETING FORM	
18 1. REPORT NUMBER USARTL-TR-78-9	2. GOVT ACCESSION NO.	3. RECIPIENT'S CATALOG NUMBER	
4. TITLE (and Subtitle) EFFECT OF OPERATIONAL ENVELOPE LIMITS ON TEETERING ROTOR FLAPPING.		5. TYPE OF REPORT & PERIOD COVERED FINAL REPORT. June 1976-August 1977	
7. AUTHOR(s) L. W./Dooley S. W./Ferguson, III		8. CONTRACT OR GRANT NUMBER(s) DAAJ02-76-C-0043/m	
9. PERFORMING ORGANIZATION NAME AND ADDRESS Bell Helicopter Textron P. O. Box 482 Fort Worth, Texas 76101		10. PROGRAM ELEMENT, PROJECT, TASK AREA & WORK UNIT NUMBERS 62209A/1L262209AH76B 00 157EK	
11. CONTROLLING OFFICE NAME AND ADDRESS Applied Technology Laboratory, U.S. Army Research & Technology Lab. (AVRADCOM) Fort Eustis, Virginia 23604		12. REPORT DATE July 1978	
14. MONITORING AGENCY NAME & ADDRESS (if different from Controlling Office) 94.		13. NUMBER OF PAGES 93	
		15. SECURITY CLASS. (of this report) UNCLASSIFIED	
		15a. DECLASSIFICATION/DOWNGRADING SCHEDULE	
16. DISTRIBUTION STATEMENT (of this Report) Approved for public release; distribution unlimited.			
17. DISTRIBUTION STATEMENT (of the abstract entered in Block 20, if different from Report)			
18. SUPPLEMENTARY NOTES			
19. KEY WORDS (Continue on reverse side if necessary and identify by block number) Rotor flapping, Rotorcraft flight simulation, Flapping in maneuvers, AH-1 Helicopter, Helicopter, Operational envelope			
20. ABSTRACT (Continue on reverse side if necessary and identify by block number) The objectives of this study were to verify the accuracy of the hybrid computer version of the Rotorcraft Simulation Program C81 as a flapping predictor, to investigate the effect of operational envelope limits on flapping, and to investigate methods of extend- ing the recommended operational envelopes of the subject heli- copter.			

DD FORM 1 JAN 73 1473 EDITION OF 1 NOV 65 IS OBSOLETE

UNCLASSIFIED

SECURITY CLASSIFICATION OF THIS PAGE (When Data Entered)

054 200

LB

UNCLASSIFIED

SECURITY CLASSIFICATION OF THIS PAGE(When Data Entered)

20. ABSTRACT: Continued

It was determined that flapping in severe maneuvers can be satisfactorily predicted using the hybrid version of C81. Flapping predictions are dependent on the interpretation of computer operator on how the pilot would move the controls during a maneuver.

Based on these simulations, the most critical operational envelope for the subject helicopter was a restriction in low-g flight. Other envelopes affected flapping, but, with the exception of center-of-gravity, these effects were relatively small. Pilot control technique was also important with large, abrupt control inputs causing increased flapping.

The most promising method of alleviating loads due to high flapping is incorporation of mast moment springs. These provide additional control power in low-g flight and reduce flapping in most flight conditions. Other possible methods involve control system modification that restrict or correct pilot inputs that may generate high flapping.

UNCLASSIFIED

SECURITY CLASSIFICATION OF THIS PAGE(When Data Entered)

PREFACE

The work reported herein was performed by Bell Helicopter Textron under Contract DAAJ02-76-C-0043, "Guidelines for Rotor Blade Flapping Limits," awarded in June 1976 by the Eustis Directorate of the U.S. Army Air Mobility Research and Development Laboratory (USAAMRDL).*

Technical program direction was provided by Mr. G. T. White of USAAMRDL. Principal Bell Helicopter Textron personnel associated with the program were L. W. Dooley, K. E. Builta, S. W. Ferguson, M. M. Joglekar, J. M. Robertson, and F. M. Schramm.



*Redesignated Applied Technology Laboratory,
U.S. Army Research and Technology Laboratories (AVRADCOM)
Fort Eustis, Virginia, 1 September 1977

TABLE OF CONTENTS

	<u>Page</u>
PREFACE.....	3
LIST OF ILLUSTRATIONS.....	7
LIST OF TABLES.....	9
1. INTRODUCTION.....	10
1.1 OBJECTIVES.....	10
1.2 TECHNICAL APPROACH.....	10
2. COMPARISON OF SIMULATION TO FLIGHT TEST.....	12
2.1 SIMULATION MODEL.....	12
2.2 SIMULATED MANEUVERS.....	13
2.2.1 Roll Reversals.....	14
2.2.2 Symmetrical Pull-up.....	21
2.2.3 Symmetrical Push-over.....	21
2.2.4 Rolling Pull-out.....	21
2.2.5 Symmetrical Flare.....	26
2.2.6 Steady Turns.....	26
2.3 RESULTS OF SIMULATION.....	30
3. AH-1 OPERATING ENVELOPE LIMITS.....	31
3.1 SIMULATION MODEL DEVELOPMENT.....	31
3.2 ENVELOPE EXPANSION SIMULATION MANEUVERS.....	32
3.2.1 Effect of Center of Gravity.....	39
3.2.1.1 High-g Maneuvers.....	39
3.2.1.2 Low-g Maneuvers.....	43
3.2.1.3 Roll Reversals.....	47
3.2.1.4 Engine Failures.....	47
3.2.2 Effect on Gross Weight.....	47
3.2.2.1 High-g Maneuvers.....	51
3.2.2.2 Low-g Maneuvers.....	51
3.2.2.3 Roll Reversals.....	51
3.2.2.4 Engine Failures.....	51

PRECEDING PAGE BLANK-NOT FILMED

70

5

102

TABLE OF CONTENTS - Concluded

	<u>Page</u>
3.2.3 Effect of Rotor Speed.....	55
3.2.3.1 High-g Maneuvers.....	55
3.2.3.2 Low-g Maneuvers.....	55
3.2.3.3 Roll Reversals.....	55
3.2.4 Effect of Power Required.....	58
3.2.4.1 High-g Maneuvers.....	58
3.2.4.2 Low-g Maneuvers.....	60
3.2.4.3 Roll Reversals.....	60
3.2.4.4 Engine Failures.....	62
3.2.5 Configuration Effects.....	63
3.3 RESULTS OF ENVELOPE LIMIT STUDIES.....	63
4. METHODS OF EXTENDING OPERATIONAL ENVELOPES.....	65
4.1 INCREASED HUB FLAPPING CLEARANCE.....	65
4.2 METHODS TO REDUCE FLAPPING USING FLIGHT CONTROLS.....	67
4.2.1 Control Rate Limiters.....	67
4.2.2 Force Feel Limiters.....	68
4.2.3 Active Flapping Controller.....	71
4.2.4 Hub Moment Restraint.....	75
4.3 STOP CONTACT LOAD ALLEVIATION.....	80
4.3.1 Thick Wall Mast.....	80
4.3.2 Mast Plug.....	86
4.3.3 Alternate Stop Locations.....	86
4.3.4 Energy Absorption Methods.....	87
4.4 RESULTS OF METHODS STUDY.....	89
5. CONCLUSIONS AND RECOMMENDATIONS.....	90
5.1 CONCLUSIONS.....	90
5.2 RECOMMENDATIONS FOR FURTHER STUDY.....	90
6. REFERENCES.....	92
7. LIST OF SYMBOLS.....	93

LIST OF ILLUSTRATIONS

<u>Figure</u>		<u>Page</u>
1	Right roll reversal at 140 knots.....	15
2	Left roll reversal at 140 knots.....	17
3	Effect of incorrect control inputs on flapping prediction in left roll reversal at 140 knots.....	19
4	Symmetrical pull-up at 140 knots.....	22
5	Symmetrical push-over at 112 knots.....	23
6	Left rolling pull-out at 140 knots.....	24
7	Symmetrical flare from 140 knots.....	27
8	Right turn at 126 knots.....	28
9	Left turn at 86 knots.....	29
10	AH-1R symmetrical pull-up at 89 knots.....	33
11	AH-1R symmetrical pull-up at 122 knots.....	34
12	AH-1G symmetrical push-over at 130 knots.....	35
13	AH-1 loading limits.....	38
14	Target load factor variation with gross weight.....	40
15	AH-1G/R simulated low-g maneuvers at 120 knots.....	44
16	AH-1G/R engine failure and recovery at 140 knots.....	49
17	Blade to fuselage clearance.....	66
18	Modified force feel system.....	69
19	Control damping force variation with control motion.....	70
20	Block diagram of the flapping controller.....	73

LIST OF ILLUSTRATIONS - Concluded

<u>Figure</u>		<u>Page</u>
21	Effect of a flapping controller in a pull-up maneuver.....	74
22	Nonlinear hub spring characteristics.....	77
23	Nonlinear hub spring design.....	77
24	Nonlinear hub spring for AH-1G/R simulation.....	78
25	The effect of a nonlinear hub spring on flapping in a push-over maneuver.....	79
26	Design flight loads for a teetering rotor helicopter.....	81
27	Mast load capabilities at the flapping stop waterline.....	82
28	Shear loading due to flapping stop contact.....	83
29	Mast load capabilities at the flapping stop waterline with stop contact.....	84
30	Effect of thick wall mast on mast load capabilities at the flapping stop waterline.....	85

LIST OF TABLES

<u>Table</u>	<u>Page</u>
1	SIMULATION MATRIX..... 37
2	AH-1G/R MAIN ROTOR RPM LIMITS..... 38
3	AH-1G/R FUSELAGE RATE AND ATTITUDE LIMITS..... 41
4	EFFECT OF CENTER OF GRAVITY ON AH-1G/R HIGH-G MANEUVERS..... 42
5	EFFECT OF CENTER OF GRAVITY ON AH-1G/R LOW-G MANEUVERS..... 46
6	EFFECT OF CENTER OF GRAVITY ON AH-1G/R ROLL REVERSALS..... 48
7	EFFECT OF CENTER OF GRAVITY ON AH-1G/R ENGINE FAILURES..... 48
8	EFFECT OF GROSS WEIGHT ON AH-1G/R HIGH-G MANEUVERS..... 52
9	EFFECT OF GROSS WEIGHT ON AH-1G/R LOW-G MANEUVERS..... 53
10	EFFECT OF GROSS WEIGHT ON AH-1G/R ROLL REVERSALS..... 54
11	EFFECT OF GROSS WEIGHT ON AH-1G/R ENGINE FAILURES..... 54
12	EFFECT OF MAIN ROTOR RPM ON AH-1G/R HIGH-G MANEUVERS..... 56
13	EFFECT OF MAIN ROTOR RPM ON AH-1G/R LOW-G MANEUVERS..... 57
14	EFFECT OF MAIN ROTOR RPM ON AH-1G/R ROLL REVERSALS..... 58
15	EFFECT OF POWER ON AH-1G/R HIGH-G MANEUVERS..... 59
16	EFFECT OF POWER ON AH-1G/R LOW-G MANEUVERS..... 61
17	EFFECT OF POWER ON AH-1G/R ROLL REVERSALS..... 61
18	EFFECT OF POWER ON AH-1G/R ENGINE FAILURES..... 63

1. INTRODUCTION

Knowledge and evaluation of rotor blade flapping is fundamental to helicopter design and operation. Reference 1 determined some basic flapping design criteria for helicopters in general and provided insight into the flapping that can be expected in both steady flight and maneuvers. Additionally, several areas requiring further study were recommended. This study addresses some of those recommendations.

1.1 OBJECTIVES

The objectives of this study were to verify the accuracy of the flapping prediction methods, to investigate the effect on flapping of operating a specific helicopter out of its recommended flight envelope, and to investigate methods of extending the recommended flight envelopes for the same helicopter.

1.2 TECHNICAL APPROACH

The Bell Helicopter Textron (BHT) Model 214A helicopter was used for the verification of prediction methods. This helicopter was chosen because of the availability of flapping data in structural demonstration-type maneuvers. The hybrid computer version of the C81 Rotorcraft Simulation Program (Reference 2) was used to simulate specific structural demonstration-type maneuvers involving large rotor blade flapping magnitudes. After establishing that this method could adequately correlate measured and predicted flapping in these maneuvers, the computer inputs were modified to simulate an AH-1 helicopter. The AH-1 was chosen to be representative of current Army helicopters. Using existing operational envelope limits as established in the operators manual (Reference 3), a series of severe maneuvers were simulated which were both within and outside the boundaries of these envelopes.

¹ L. W. Dooley, ROTOR BLADE FLAPPING CRITERIA INVESTIGATION, USAAMRDL Technical Report 76-33, Eustis Directorate, U.S. Army Air Mobility Research and Development Laboratory, Fort Eustis, Virginia, December 1976, AD A034459.

² J. M. Davis, et al., ROTORCRAFT FLIGHT SIMULATION WITH AERO-ELASTIC ROTOR AND IMPROVED AERODYNAMIC REPRESENTATION, USAAMRDL Technical Report 74-10A,B,C, Eustis Directorate, U.S. Army Air Mobility Research and Development Laboratory, Fort Eustis, Virginia, June 1974, AD782854, 782756, 782841.

³ Anon, OPERATORS MANUAL, ARMY MODEL AH-1G HELICOPTER, TM55-1520-221-10, Headquarters, Department of the Army, May 1975.

Several promising methods to extend the operational envelopes of the AH-1 helicopter were then analyzed to determine effectiveness in reducing flapping and in application to existing helicopters.

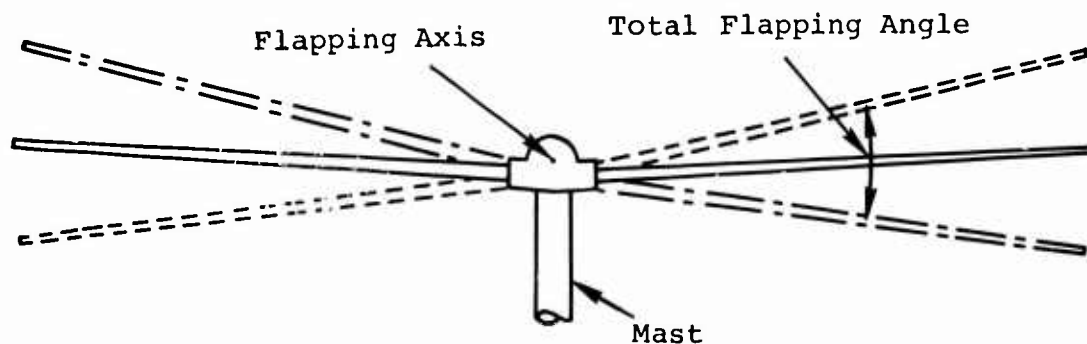
The flapping prediction verification is presented in Section 2, the operational limits study in Section 3, and the methods of extending the operational envelopes in Section 4.

2. COMPARISON OF SIMULATION TO FLIGHT TEST

The accuracy of the hybrid version of the Rotorcraft Flight Simulation Program (C81) in the prediction of main rotor flapping was demonstrated through the simulation of selected maneuvers of the BHT Model 214A helicopter. The flight test records chosen were based upon high flapping peaks and data availability. The maneuvers simulated were performed during the structural demonstration (Reference 4) and handling qualities (Reference 5) test programs. The six types of maneuvers simulated were: (1) roll reversals, (2) symmetrical pull-up, (3) symmetrical push-over, (4) symmetrical flare from V_{NE} to hover, (5) coordinated windup turns, and (6) rolling pull-outs.

2.1 SIMULATION MODEL

The BHT Model 214A helicopter was modeled for the hybrid computer version of the Rotorcraft Flight Simulation Program (C81), described in Reference 2. This model represents a two-bladed teetering rotor helicopter with rigid blades. As seen in the sketch below, the flapping output of C81 is the angle that the teetering hub makes with the plane perpendicular to the main rotor mast, which corresponds to flight test measurements (100 percent flapping equals ± 10 degrees).



⁴R. A. Magnuson, STRUCTURAL DEMONSTRATION RESULTS FOR THE IRANIAN MODEL 214A HELICOPTER, Bell Report No. 214-099-079, Bell Helicopter Textron, Ft. Worth, Texas, April 3, 1975.

⁵J. T. Blaha, HANDLING QUALITIES DEMONSTRATION OF THE IRANIAN MODEL 214A HELICOPTER, Bell Report 214-099-081, Bell Helicopter Textron, Ft. Worth, Texas, February 24, 1975.

In the simulation, the blades are assumed to be rigid. The hybrid computer simulation output is available as an on-line time history plot of selected parameters and, at maneuver times specified by the user, a printed summary of variables listed similarly to the trim page output of the digital version of C81. If a particular maneuver is saved on magnetic tape, a computer-generated plot of any calculated parameter may be obtained. All three types of output were used for this simulation work.

2.2 SIMULATED MANEUVERS

Each maneuver, with the exception of the coordinated turns, was simulated using the following technique. A time history of the pertinent fuselage rates, attitudes, and g-level was transferred to translucent paper using the same scales as the hybrid on-line time history plots. Using the flight test control inputs as a starting point, control motions were specified and the maneuver was simulated. The time histories produced by the hybrid were compared with the flight test data by overlaying the translucent plots. The hybrid control motions were then adjusted as necessary and the maneuver was repeated until a satisfactory comparison with flight gyro and load factor test data were obtained. In no cases were the maximum control input rates for flight test data exceeded; only the magnitude of the control inputs were varied. These maneuvers were simulated with SCAS ON.

Maneuvers examined in this study were roll reversals, pullups, pushovers, flares, coordinated turns, and rolling pullouts. The main rotor hub flapping peaks were predicted to within less than one degree of the measured flight test results for all of the simulated maneuvers. These results are also reported in Reference 6.

⁶L. W. Dooley, COMPARISON OF HYBRID C81 SIMULATION TO FLIGHT TEST RESULTS FOR MANEUVERS CAUSING LARGE FLAPPING, Bell Report 699-099-032, Bell Helicopter Textron, Ft. Worth, Texas, October, 1976.

2.2.1 Roll Reversals

The roll reversal maneuvers were initiated from a stabilized level flight condition by supplying control inputs as required to obtain a bank angle of at least 45 degrees to the right or left. From this bank angle, a rapid lateral cyclic control input was used to generate a roll rate of at least 60 degrees per second in the direction to reduce the bank angle. When the peak roll rate was obtained, a lateral cyclic input was introduced in the opposite direction to reduce the roll rate to zero.

The left and right roll reversals which were simulated are presented in Figures 1 and 2, respectively. Using the left roll reversal as an example, there are basically two flapping peaks of main interest. The first flapping peak (at about 7 seconds on Figure 2) is generated immediately after the control input commanding the 60-degree-per-second roll rate. The second and largest peak results from the recovery input as the 60-degree-per-second rate is attained. The second input resulted in higher flapping because of a combination of the larger commanded swashplate angle and rotor lag associated with roll rate.

In correlating the roll reversal maneuvers, as well as the other maneuvers, it was determined that accurate flapping prediction requires the fuselage angular accelerations to be matched precisely. This requires a reasonably close match of the control input time history.

To illustrate the necessity of matching the pilot control motions, an early attempt at simulating the left roll reversal is presented in Figure 3. Even though the fuselage attitudes and rates were matched reasonably well, the lateral cyclic stick motion did not match the flight test records and consequently the flapping peaks were predicted incorrectly.

When correlating flapping with previously performed flight test maneuvers, the control technique used by the pilot may be duplicated and flapping peaks predicted accurately. However, when predicting flapping in maneuvers that have not yet been flown, the accuracy of the prediction will be a direct function of how well the simulation control technique matches the control input that is used in performing the flight test maneuver.

M214A
GW = 10500 lb
CG = 134.5 in.

100% Flapping = ± 10 deg

----- C81
—— Flight Test

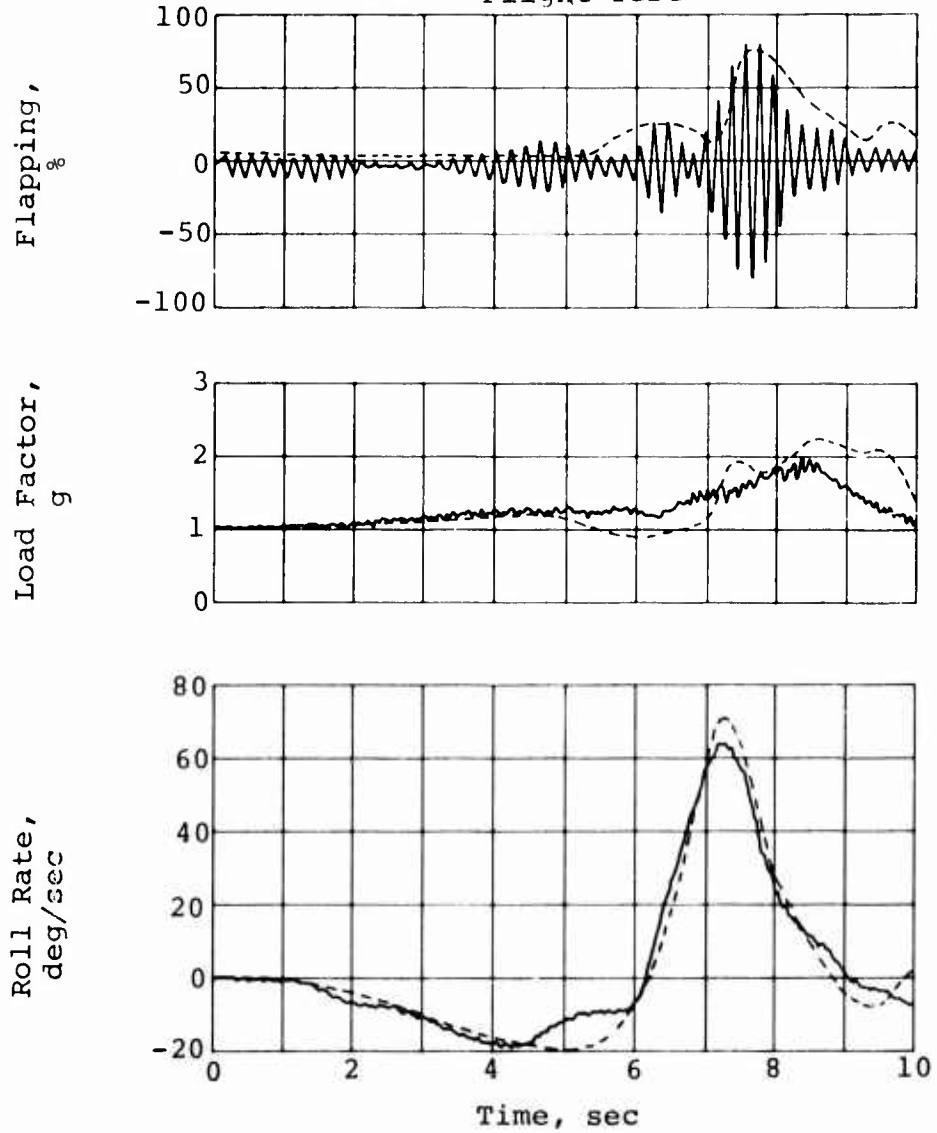


Figure 1. Right roll reversal at 140 knots.

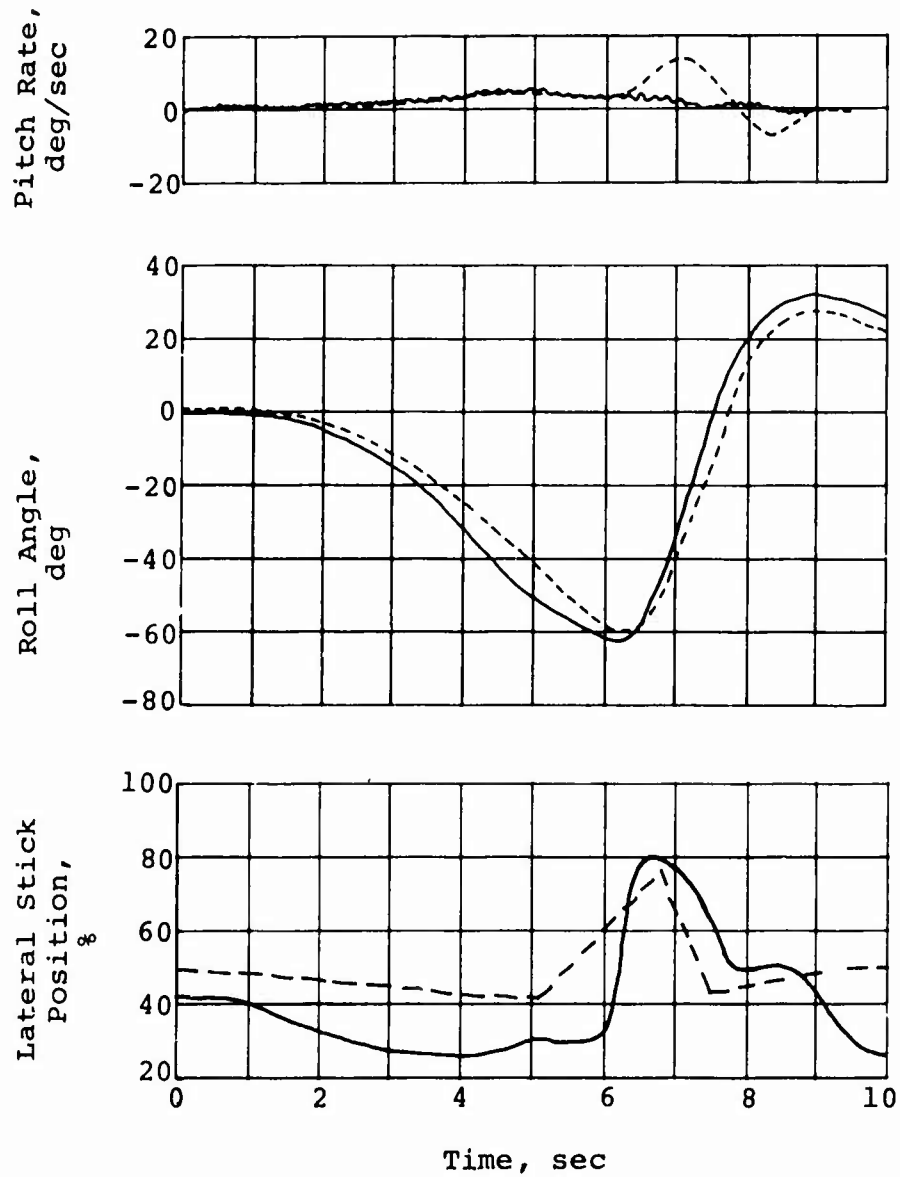


Figure 1. Concluded.

M214A
GW = 10500 lb
CG = 134.5 in.

100% Flapping = ± 10 deg

----- C81
———— Flight Test

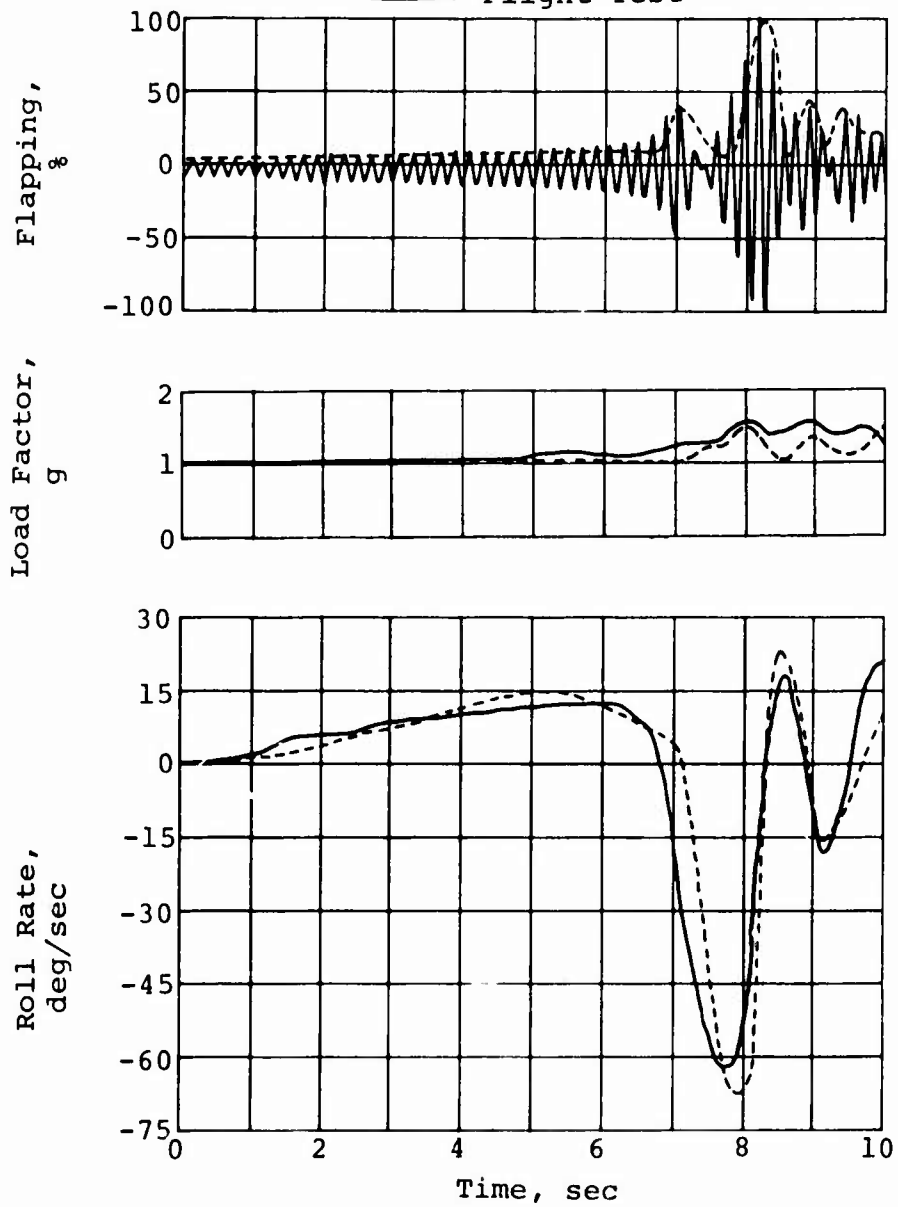


Figure 2. Left roll reversal at 140 knots.

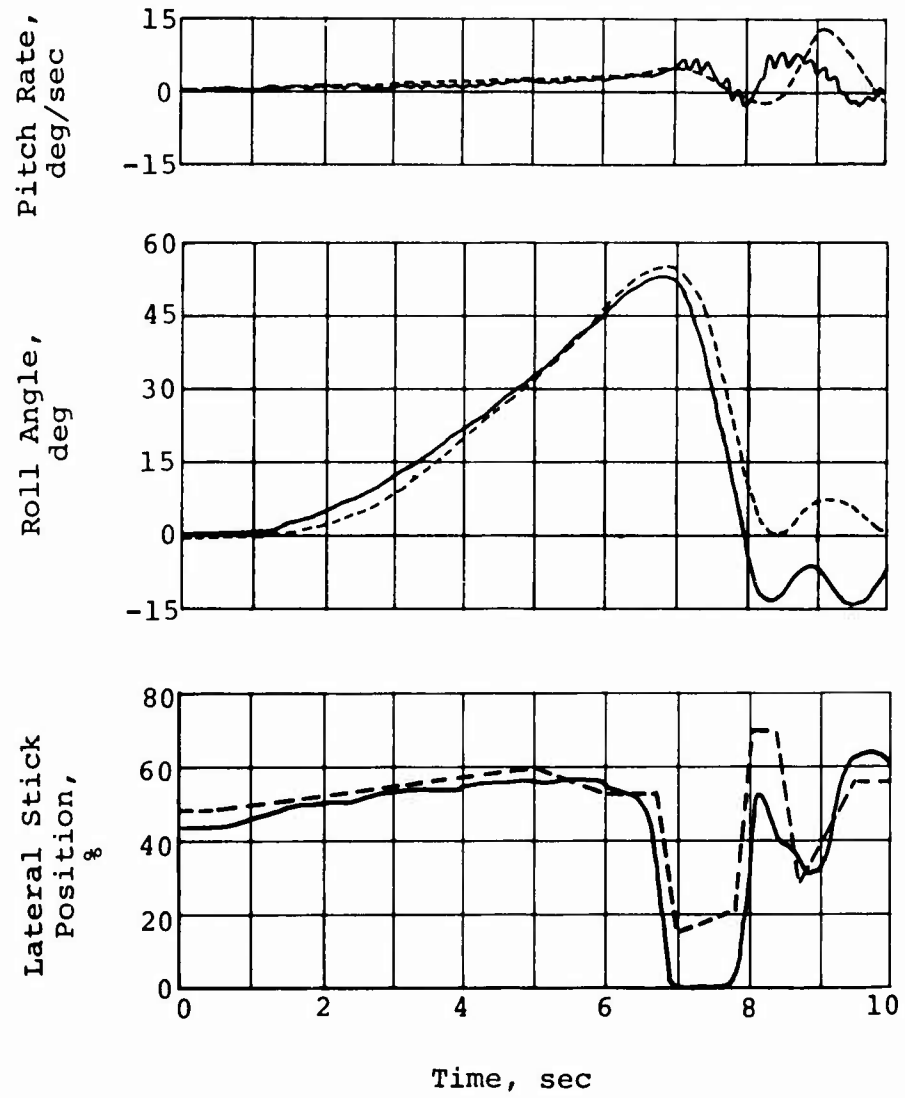


Figure 2. Concluded.

M214A
GW = 10500 lb
CG = 134.5 in.

100% Flapping = ± 10 deg
----- C81
———— Flight Test

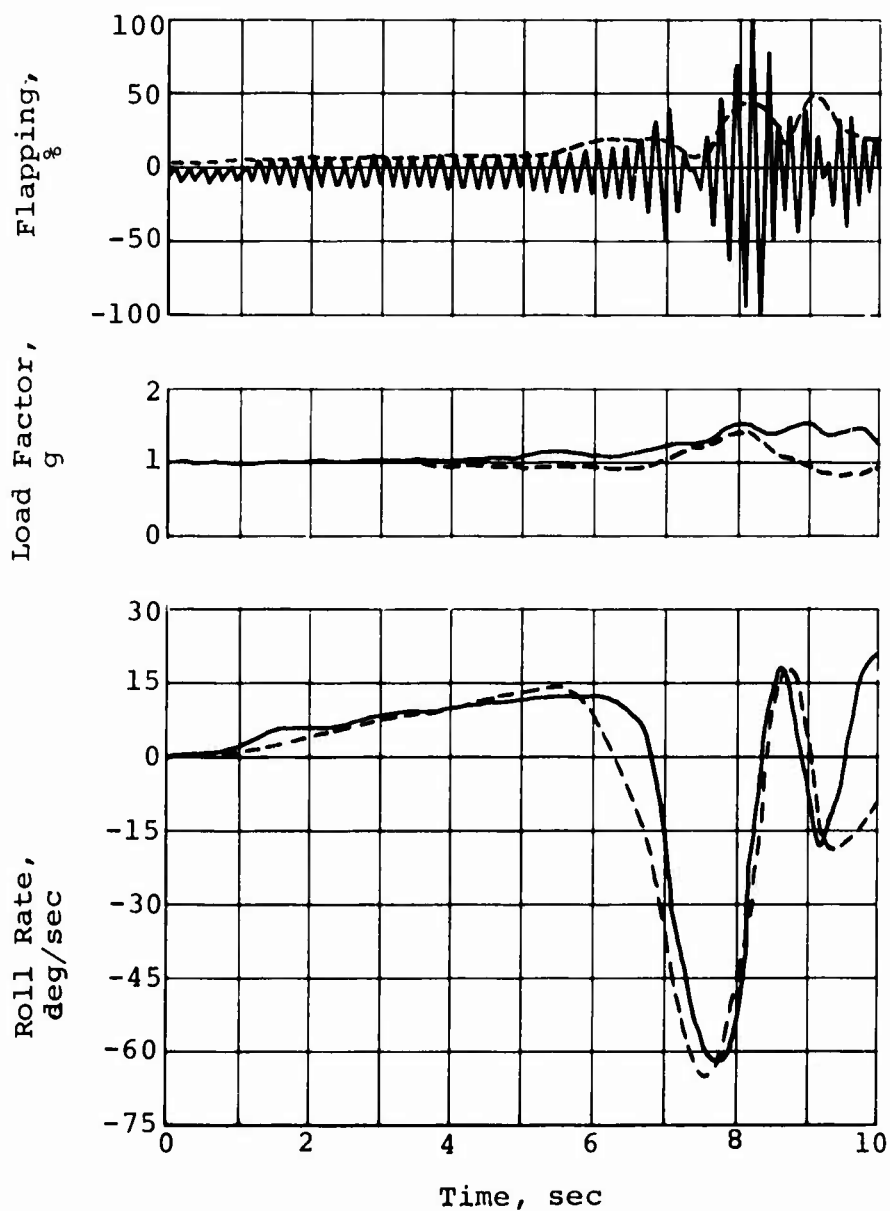


Figure 3. Effect of incorrect control inputs on flapping prediction in left roll reversal at 140 knots.

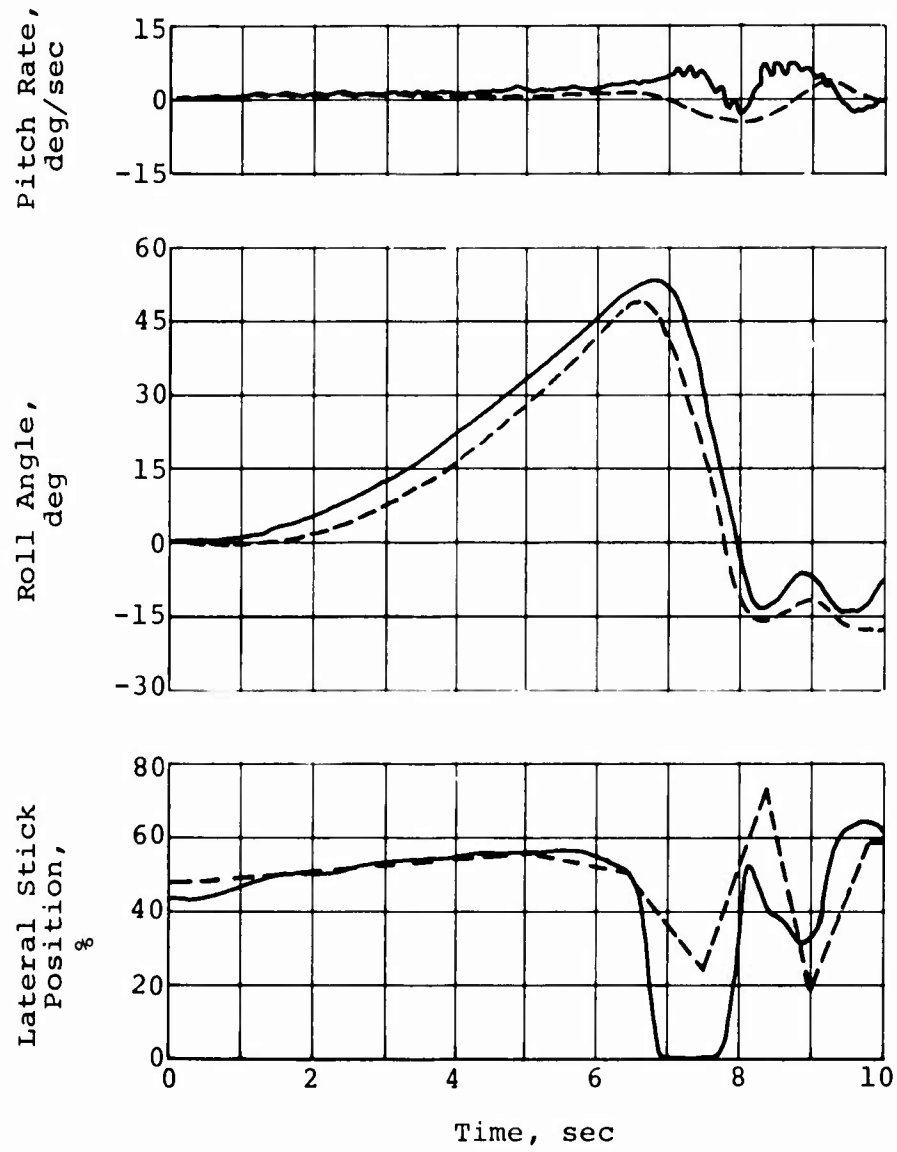


Figure 3. Concluded

2.2.2 Symmetrical Pull-Up

The symmetrical pull-up maneuver was performed from level flight entry at 140 knots using a sharp aft cyclic input to obtain a g-level of about 2.6g. The predicted peak value of flapping was within one-half of a degree of the flight test data point. Results from this maneuver are presented in Figure 4. Two flapping peaks in the maneuver occurred immediately after the initial control input and also immediately following the recovery control input. The magnitudes of the two control inputs were 27 and 23 percent of full throw, respectively. Notice again that, as was shown for roll reversals, the second peak (recovery peak) was the higher.

2.2.3 Symmetrical Push-Over

The symmetrical push-over maneuver was entered from level flight at 112 knots. The control inputs were the almost simultaneous movement of longitudinal cyclic stick to the forward stop and collective to full down. This resulted in a momentary g-level of approximately -0.5g. This technique produces low-g conditions with a minimum of nose-down pitch rate. Flapping was predicted to within one degree for this maneuver. The results are presented in Figure 5. The narrowly spaced flapping peaks occurred immediately after the forward cyclic and down collective control inputs reached their respective full throw values. The inputs were not completed at the same time and this resulted in the two-peak trace for this maneuver.

2.2.4 Rolling Pull-Out

The rolling pull-out maneuver was performed from a level flight entry at 140 knots. The helicopter was rolled approximately 45 degrees to the right and then rolled back to level attitude at a roll rate of about 10 degrees per second. As the bank angle approached zero, a sharp aft cyclic control input was made which generated a g-level of approximately 2.5g. For the left rolling pull-out (Figure 6), the initial flapping peak, occurring during the initial cyclic longitudinal input, was predicted lower than was measured in flight test by approximately 2 degrees. The recovery peak was predicted to within one-half of a degree of flight test measurement. This maneuver, which involved simultaneous motion about both the longitudinal and lateral axes, is more time consuming to simulate than the other maneuvers of this section. Consequently, once the maximum initial and recovery flapping peak magnitudes were predicted, no further refinement of this maneuver was attempted.

M214A
 GW = 10500 lb
 CG = 135.0 in.

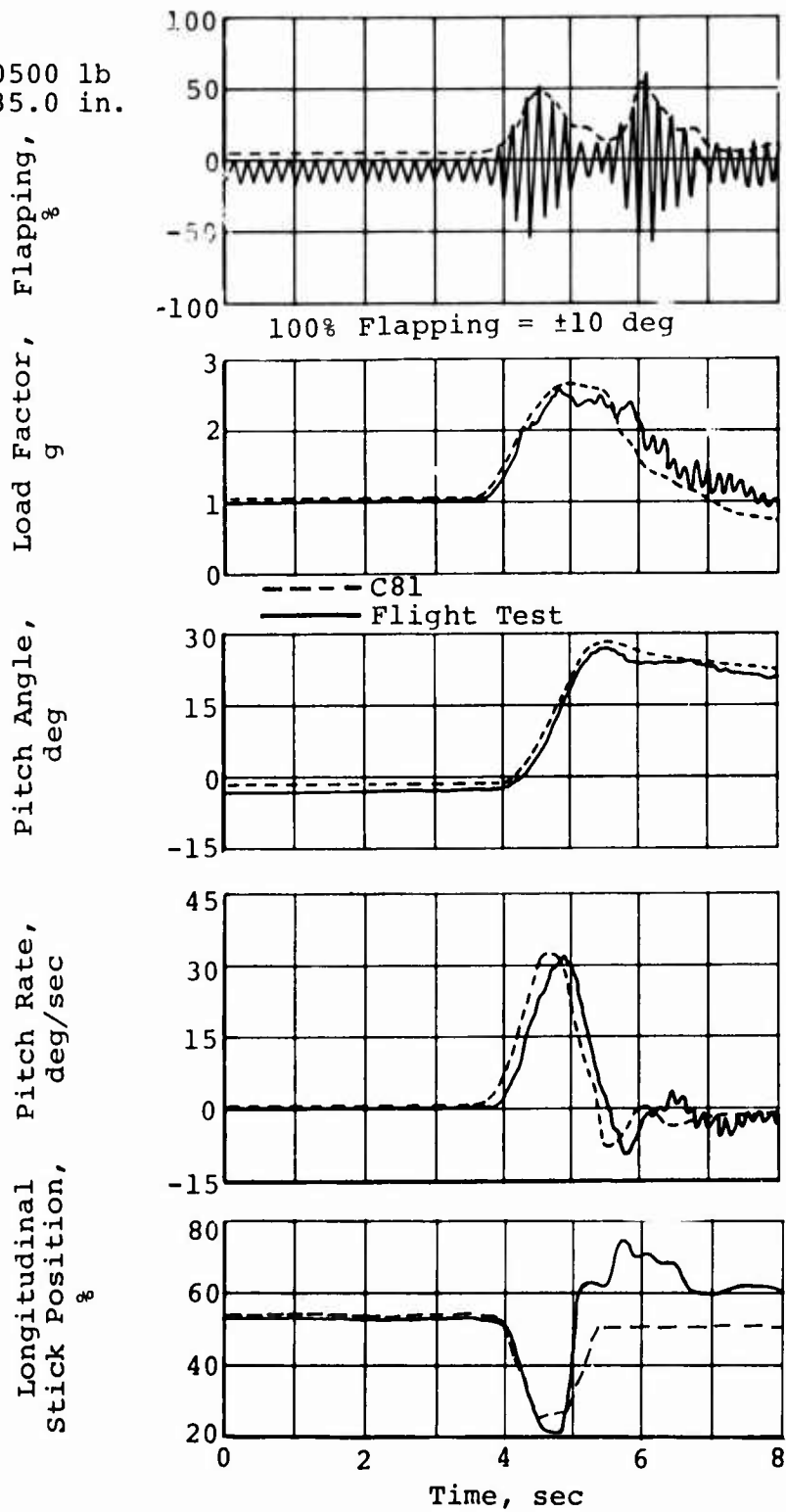


Figure 4. Symmetrical pull-up at 140 knots.

M214A
 GW = 10500 lb
 CG = 134.5 in.

100% Flapping = ± 10 deg
 --- C81
 — Flight Test

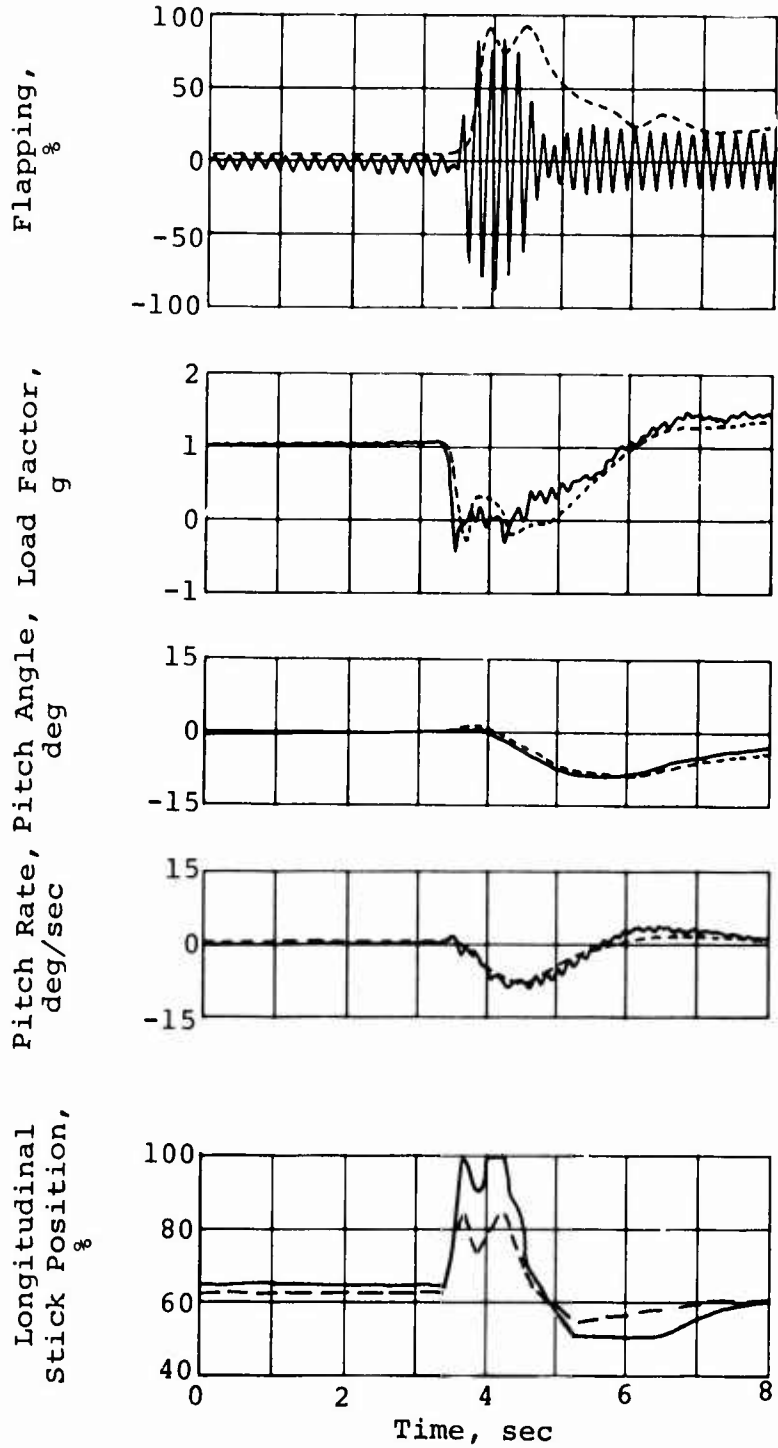


Figure 5. Symmetrical push-over at 112 knots.

M214A

GW = 10500 lb
CG = 134.5 in.

100% Flapping = ± 10 deg

--- C81
— Flight Test

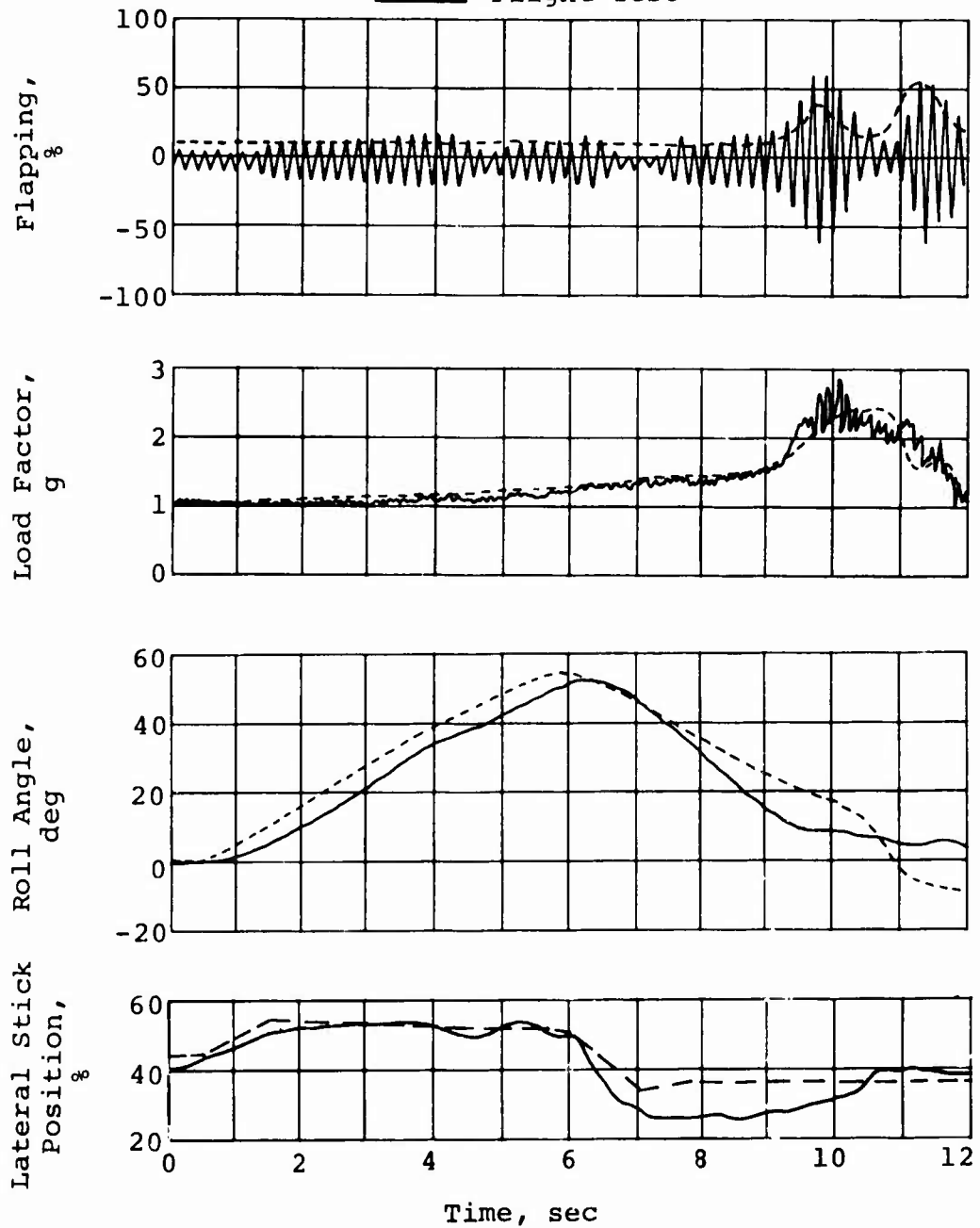


Figure 6. Left rolling pull-out at 140 knots.

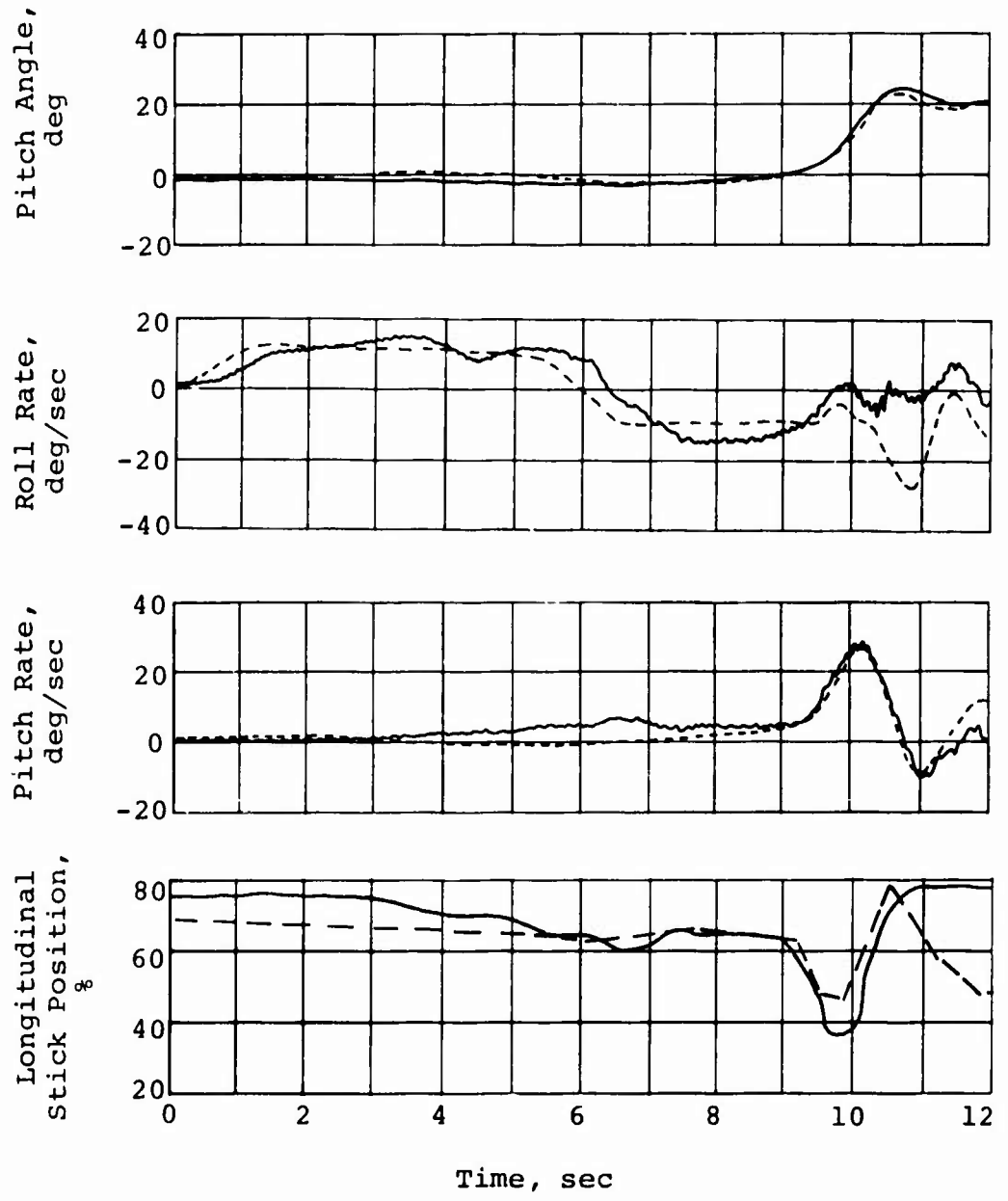


Figure 6. Concluded.

2.2.5 Symmetrical Flare

A symmetrical flare was found in the initial portion of a quick-stop maneuver presented in Reference 4. This maneuver was a maximum performance deceleration from 140 knots to hover at approximately constant altitude. The maneuver was started with an aft longitudinal cyclic control input to flare to approximately 20° nose-up attitude which was held throughout the deceleration. Collective was dropped early in the maneuver to prevent an excessive altitude gain during the deceleration.

The simulation of the flare portion of this maneuver is presented in Figure 7. Peak flapping was predicted to within one-half degree of the measured flight test values.

2.2.6 Steady Turns

Flight test data for coordinated wind-up turns to over 1.8 g were available from the maneuvering stability tests reported in the Model 214 handling qualities tests of Reference 5. The test procedure used was to stabilize in level flight at the desired airspeed and, holding the collective stick fixed, turn in the desired direction while descending to maintain constant airspeed. Steady-state data were recorded at several g-levels during the turn. The same technique was used in generating the hybrid C81 maneuver. Flight test and simulation results of the wind-up turn maneuver are presented in Figures 8 and 9.

For a right wind-up turn at 126 knots, Figure 8, C81 matches the main rotor flapping, pitch rate, bank angle, and longitudinal cyclic stick positions in both magnitude and trends with increasing g-level. A constant one-half degree difference in main rotor flapping between flight test and C81 is held for all g-levels compared.

However, a similar maneuver to the left at 86 knots, Figure 9, does not agree as well. While pitch rate and bank angle match, C81 predicts a higher rate of flapping increase with g-level and a lower rate of longitudinal cyclic required with g-level. Unfortunately, no flight records of both right and left turns at the same airspeed and loading conditions were available to determine whether the simulation differences were a function of airspeed or of turn direction. Since the left turn simulation attained the same pitch rate and bank angle as flight test, the total forces acting on the helicopter were apparently matched. It is suspected that the representation of the elevator airflow environment or incidence caused too small a pitch rate contribution from the elevator requiring more rotor flapping than indicated in flight test.

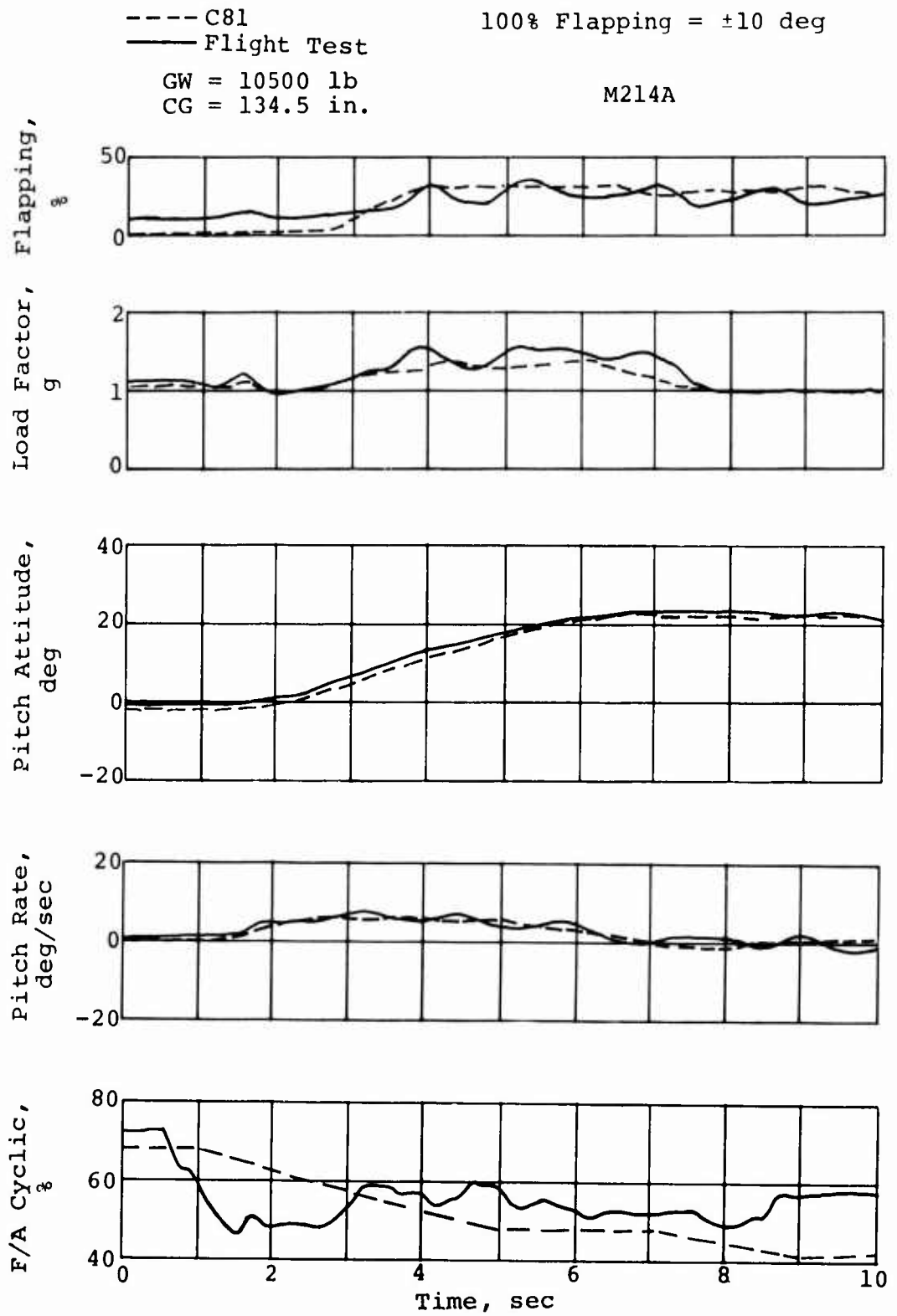


Figure 7. Symmetrical flare from 140 knots.

M214A

--- C81
— Flight Test

GW = 12500 lb
CG = 132.5 in.

100% flapping = ± 10 deg

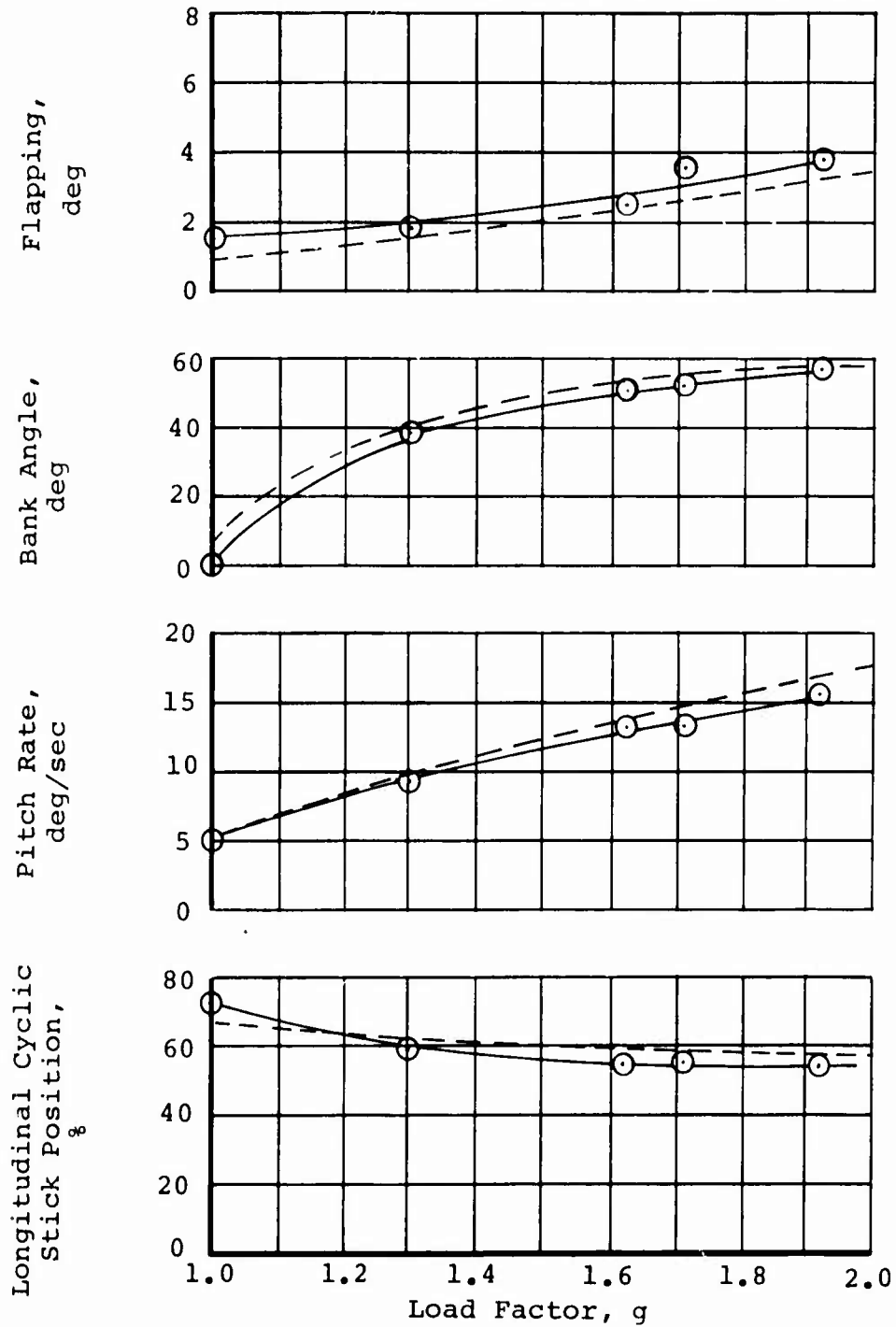


Figure 8. Right turn at 126 knots.

M214A

----- C81
—— Flight Test

GW = 12500 lb
CG = 132.5 in.

100% flapping = ± 10 deg

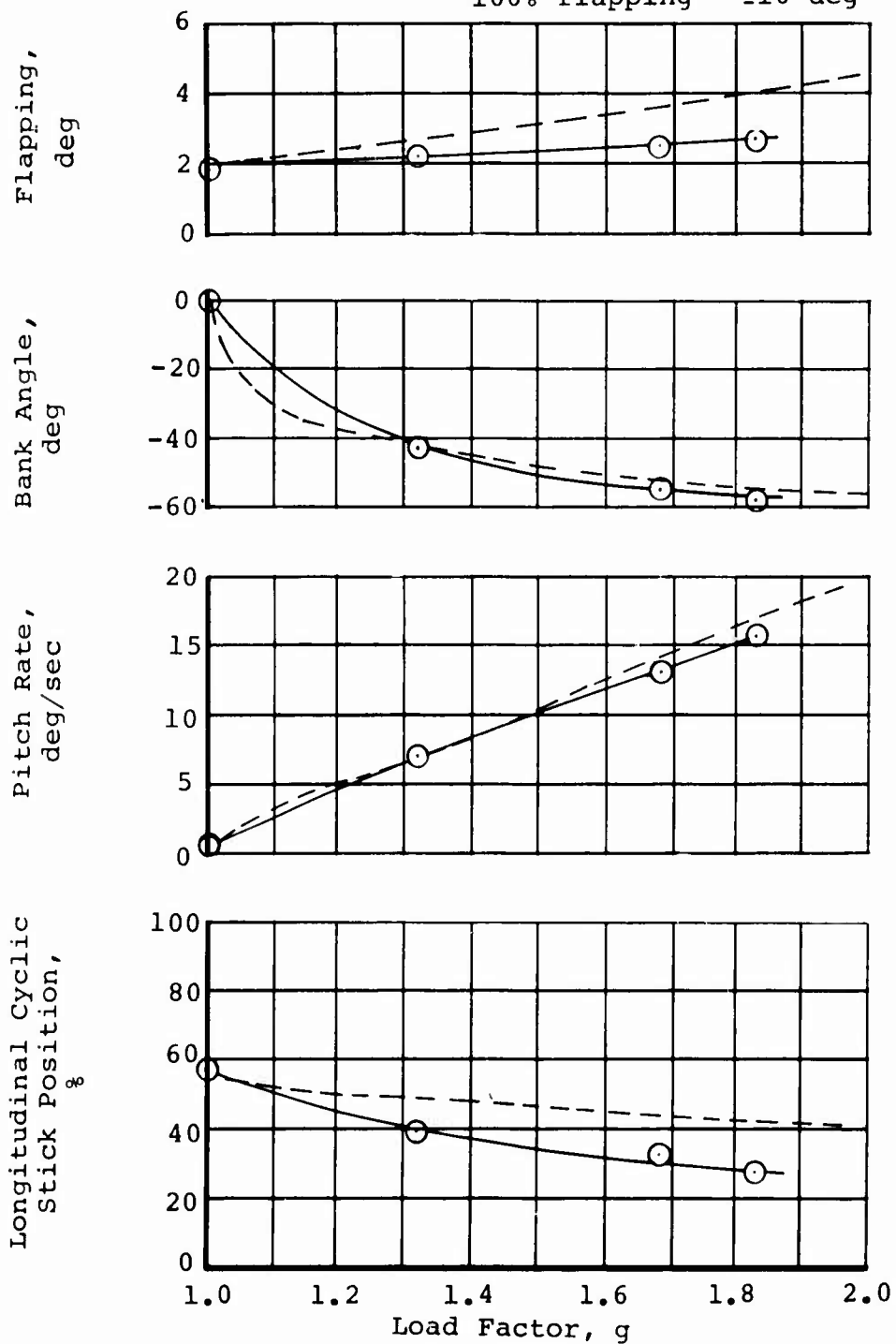


Figure 9. Left turn at 86 knots.

2.3 SUMMARY OF SIMULATION

Hybrid C81 will satisfactorily predict main rotor flapping peaks in severe maneuvers. When correlating with previously performed flight test maneuvers, calculated flapping matches test results well if the time histories of control inputs, fuselage rates and attitudes, and load factor are duplicated.

Flapping prediction in maneuvers for which prior data are unavailable will depend on the ability of the simulation operator to supply the realistic pilot inputs necessary to generate the desired helicopter motions.

3. AH-1 OPERATING ENVELOPE LIMITS

In order to evaluate the effect of operational envelopes on main rotor flapping in maneuvers, the AH-1 helicopter was simulated using hybrid C81. Only limited main rotor flapping data are available for this helicopter, but performance and maneuvering characteristics under a wide variety of operational conditions are documented. These data are available for the AH-1G and AH-1R helicopters. The differences between these two versions of the AH-1 which affect flapping are an increased gross weight limit and increased power available for the AH-1R. This allows a single simulation model (denoted AH-1G/R) to represent both helicopters.

This study consisted of first generating a suitable hybrid C81 simulation and then correlating with flight test data. Once the simulation model results were representative of flight test data, this model was used to explore the operational envelope limits of the AH-1 helicopter. Four types of flight conditions were simulated during this investigation: (1) high-g maneuvers, (2) low-g maneuvers, (3) roll reversals, and (4) engine failures. These four types of maneuvers were evaluated as functions of gross weight, center of gravity, main rotor rpm, engine power, and helicopter configuration.

3.1 SIMULATION MODEL DEVELOPMENT

The AH-1G/R simulation model was correlated with flight test data from References 7 and 8. The first of these references is the AH-1R structural demonstration report; the second is the AH-1G low-g maneuver investigation report. Three maneuvers were simulated for correlation purposes using the AH-1G/R model. These maneuvers were a pull-up at 89 knots, a pull-up at 122 knots, and a push-over at 130 knots, and were chosen primarily because those specific maneuvers were well documented in flight test. Also, the response of the model to engine failure was

⁷J. T. Blaha, STRUCTURAL DEMONSTRATION RESULTS FOR THE ICAM PROGRAM, Bell Report 209-099-415, Bell Helicopter Textron, Ft. Worth, Texas, May 23, 1975.

⁸J. R. Melton, RESULTS OF THE FLIGHT TEST INVESTIGATION OF THE REDUCED-G MANEUVER IN THE AH-1G HELICOPTER, Bell Report 209-099-309, Bell Helicopter Textron, Ft. Worth, Texas, October 3, 1969.

evaluated and compared with the test results of Reference 9. Similar fuselage attitudes, rates, and response times were then predicted with the simulation model using techniques similar to those employed in the Model 214A simulation.

The pull-up maneuvers are presented in Figures 10 and 11. Flapping was predicted accurately by hybrid C81 for both of these maneuvers. A 50-percent flapping peak (100 percent flapping equals ± 12.5 degrees) resulted from a longitudinal cyclic control input at the beginning of the 89-knot pull-up. The second peak resulted from a collective stick input. This was introduced to increase the g-level for this structural maneuver and the peak flapping reached approximately 55 percent.

The difference in flapping magnitudes for the 122-knot maneuver resulted from a trimmed pitch attitude difference of slightly more than one degree between the simulation and flight test. One degree change in pitch attitude results in approximately 8 percent change of flapping magnitude. This change in trim attitude was unidentifiable as to the exact cause. Possible areas that it could be attributed to are inaccurately labeled flight test data records, flight test instrumentation, or computer math model. This shift was not considered important since the flight test and simulation trends were very similar.

The low-g maneuver was simulated by introducing an aft cyclic input to obtain a nose-up pitch attitude and a load factor of slightly more than one. From this flight condition, the cyclic was pushed forward to obtain a load factor of 0.2g. The results matched flight test data and these results are presented in Figure 12. The flapping peak reached approximately 50 percent or ± 6 degrees at about 3 seconds. The lateral control inputs, which, as reported in Reference 2, are the primary cause of peak flapping in low-g, were introduced gradually in this maneuver and this resulted in the lack of a distinct flapping peak.

3.2 ENVELOPE EXPANSION SIMULATION MANEUVERS

Once the hybrid C81 model adequately represented the AH-1, the envelope expansion simulation was performed. The four types of maneuvers simulated in this task were: (1) high-g maneuvers, (2) low-g maneuvers, (3) roll reversals, and (4) engine failures. The high-g and low-g maneuvers were investigated as symmetrical maneuvers using cyclic only and cyclic plus collective inputs;

⁹B. M. Nicholson and M. W. Buss, AH-1G (HUEYCOBRA) HELICOPTER AUTOROTATIONAL ENTRY CHARACTERISTICS, USAASTA Project No. 70-25, U.S. Army Aviation Systems Test Activity, Edwards Air Force Base, California, April 1971.

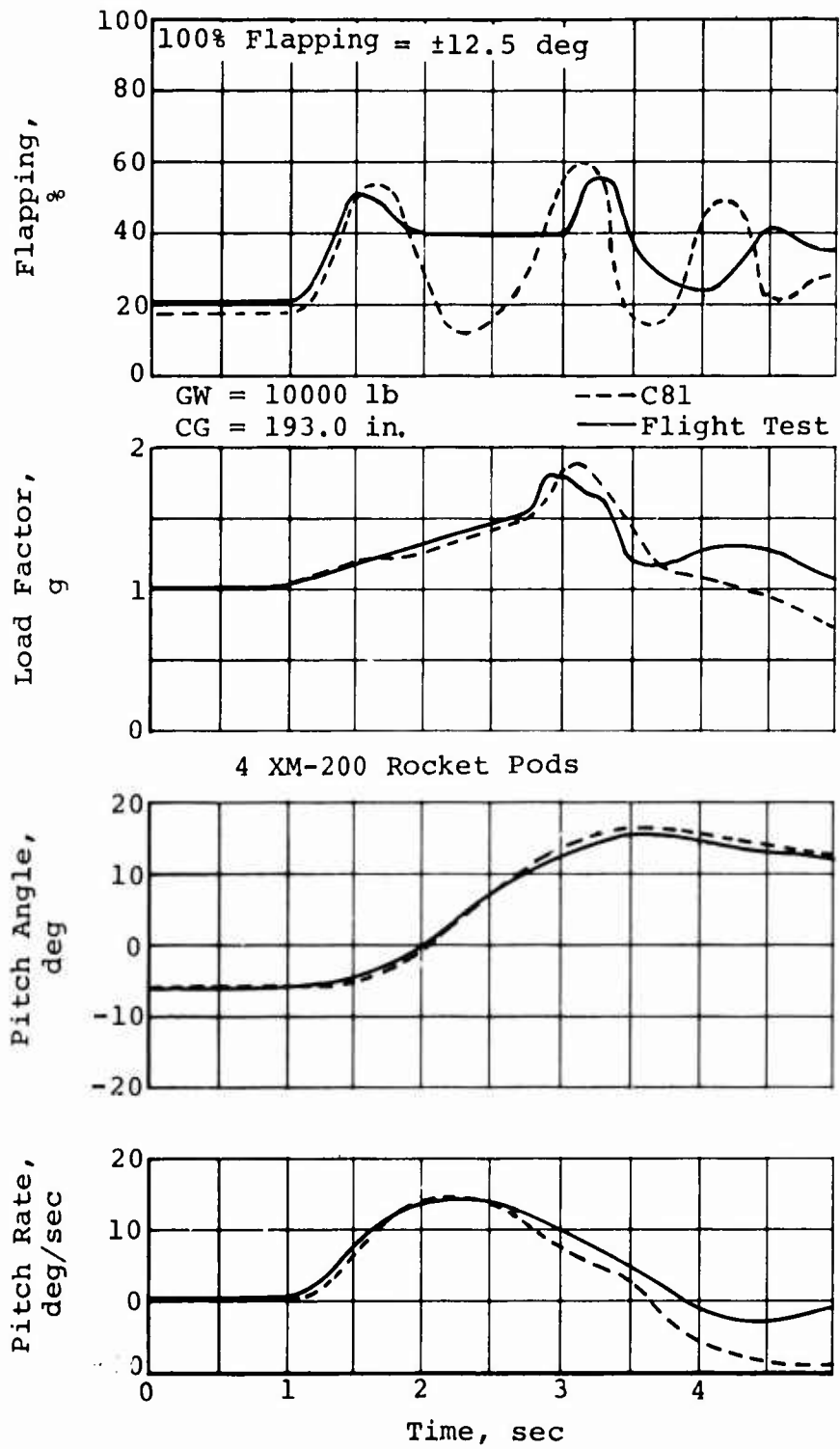


Figure 10. AH-1R symmetrical pull-up at 89 knots.

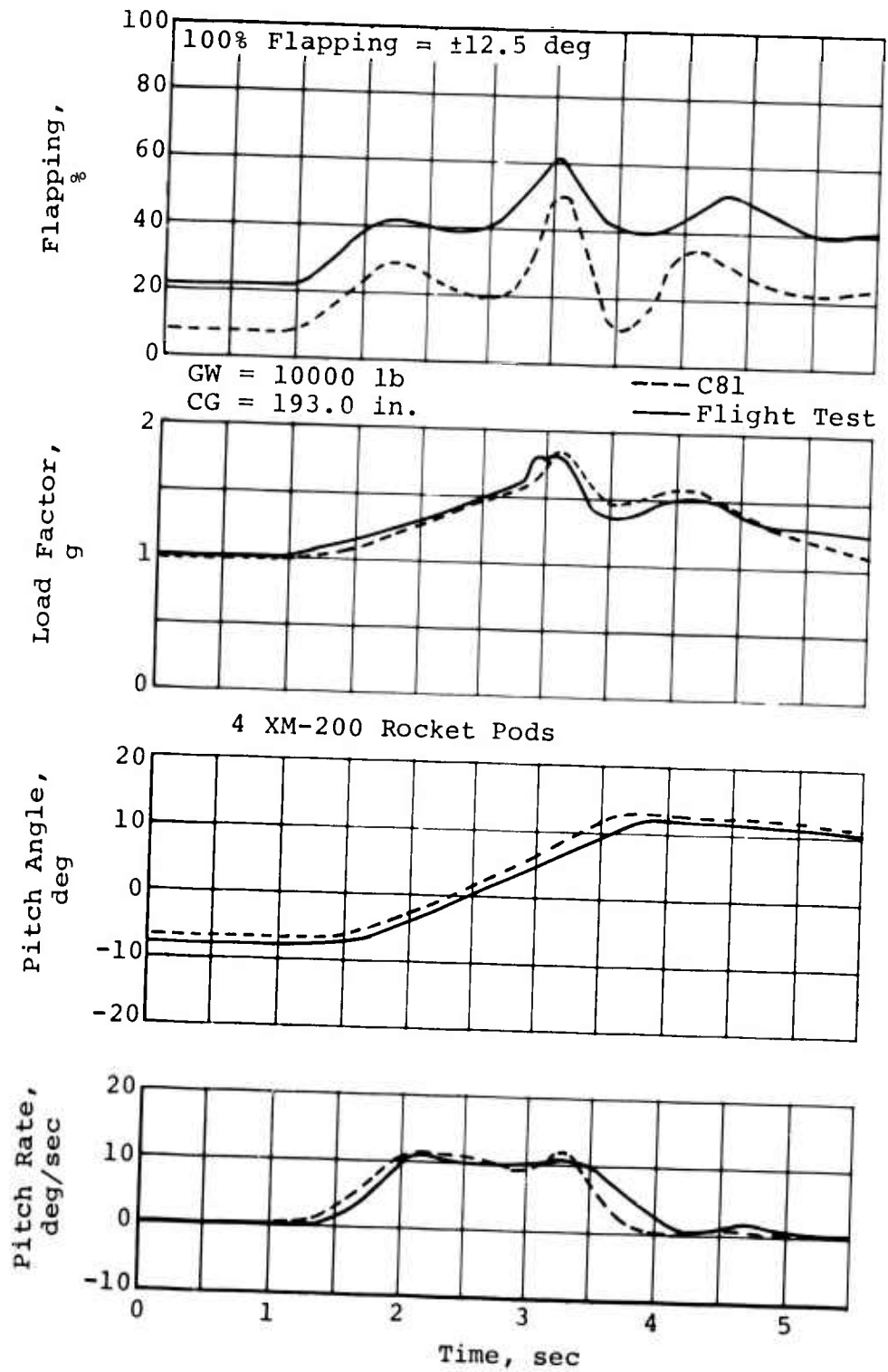


Figure 11. AH-1R symmetrical pull-up at 122 knots.

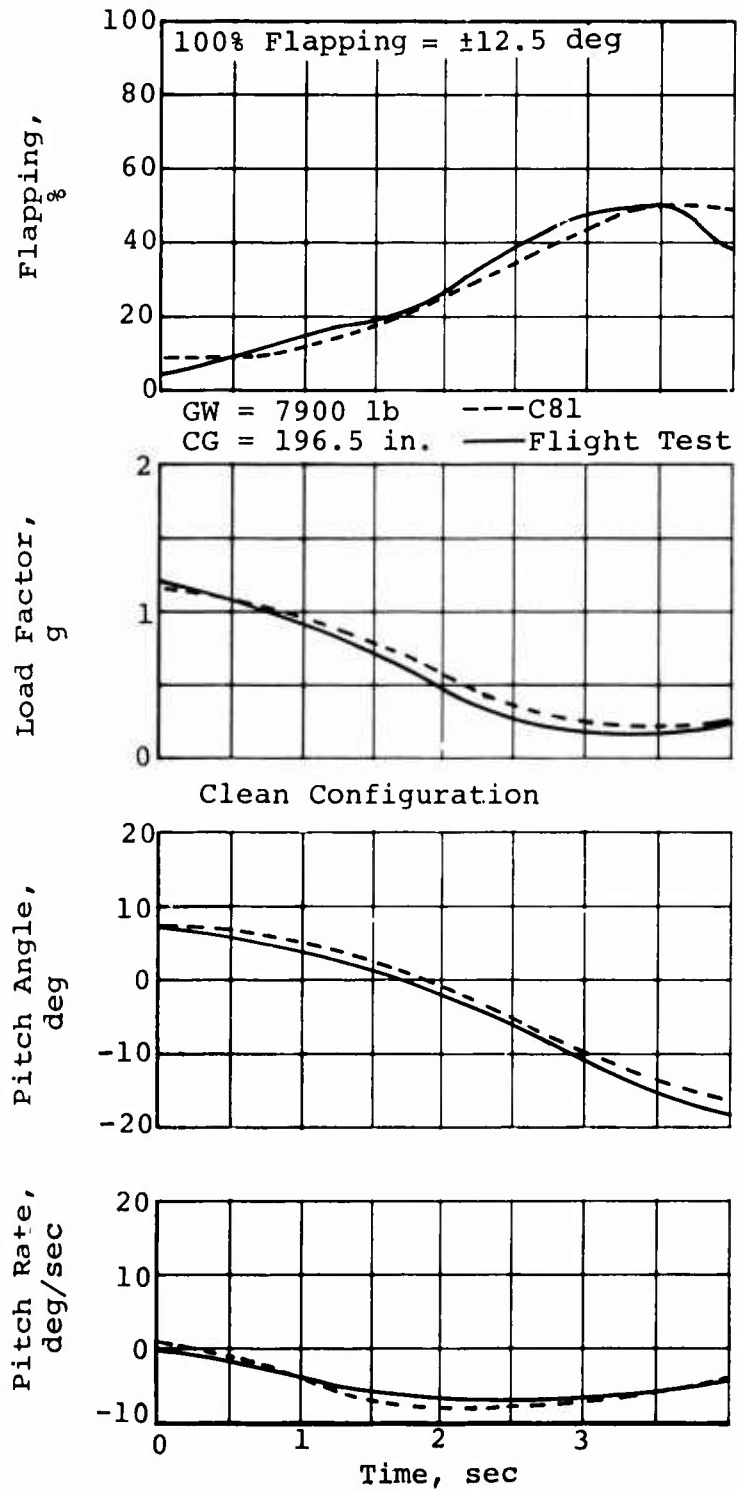


Figure 12. AH-1G symmetrical push-over at 130 knots.

and as unsymmetrical maneuvers performed from a coordinated turn. These four types of maneuvers were evaluated as functions of gross weight, center of gravity, main rotor rpm, engine power, and helicopter configuration. All of these maneuvers, except the engine failures, were simulated at 120 knots. The engine failures were simulated at 140 knots since high rotor torque values represented the worst case for engine failure.

The maneuver matrix of Table 1 presents the outline of maneuvers that were investigated along with the associated computer run number. Published gross weight, center of gravity, and main rotor rpm envelopes of the AH-1G and AH-1R are presented in Figure 13 and Table 2. The differences between the G and R models which affect flapping are an increased gross weight limit and increased power available for the AH-1R. Another operating limit appears in the operator's manual (Reference 3) prohibiting flight near or below zero g. This envelope limit is considered in the low-g portion of the simulation.

Guidelines for the simulation of these maneuvers are listed below:

1. Target values of fuselage rate, attitude, and g-level must be attained within a given time increment.
2. Control inputs introduced to attain these targets were not to exceed 100% in one-half second.
3. Each maneuver was initiated at baseline conditions with a recovery to near that of stabilized flight.
4. From the baseline condition, single-envelope parameters were exceeded in steps and the basic maneuver was repeated until the most critical flapping phase of the augmented basic maneuver was identified.

The high-g maneuvers were simulated to a constant blade loading coefficient t_c equal to 0.3 unless the pitch attitude or pitch rate magnitudes became unrealistic. The t_c of 0.3 was picked as the target blade loading because this value represented the upper limits which have been achieved consistently on the AH-1 rotor in flight test (Reference 10). The g-levels associated

¹⁰C. D. Wells and T. L. Wood, MANEUVERABILITY - THEORY AND APPLICATION, Journal of the American Helicopter Society, January 1973.

TABLE 1. SIMULATION MATRIX

	High-g			Low-g			Roll		
	Cyclic Only	Cyclic and Col-lective	Unsymmetrical	Cyclic Only	Cyclic and Col-lective	Unsymmetrical	Right	Left	Engine Failures
Center of Gravity	10	14	16	18					
	186	190	196*	201	205	21	24	26	28
	11	15	17	19	2	4	7	8	9
	1	2	3	4	5	6	23	25	27
	12	20	22	23	22	23	25	27	29
	13	21							
	30	34	35	36	37	40	41	42	43
12000 lb	31	34	35	36	37	40	41	42	44
11000 lb	32								
10000 lb	1	2	3	4	5	6	7	8	9
8000 lb*	33								
6000 lb	33								
	45	48	49	50	51	53	54	55	57
339	46	48	49	50	51	53	54	55	57
324*	1	2	3	4	5	6	7	8	9
294	47								
274	47								
	59	61	62	63	64	66	67	68	69
1290	60	61	62	63	64	66	67	68	69
Engine Power	1	2	3	4	5	6	7	8	9
As Required*	0	61	62	64	64	66	67	68	69
	70	71	72	73	74	75	76	77	78
Clean	70	71	72	73	74	75	76	77	78
Config-uration	1	2	3	4	5	6	7	8	9
Wing Stores*	1	2	3	4	5	6	7	8	9

*Baseline Conditions
 Note: Numbers indicate computer run identification number.

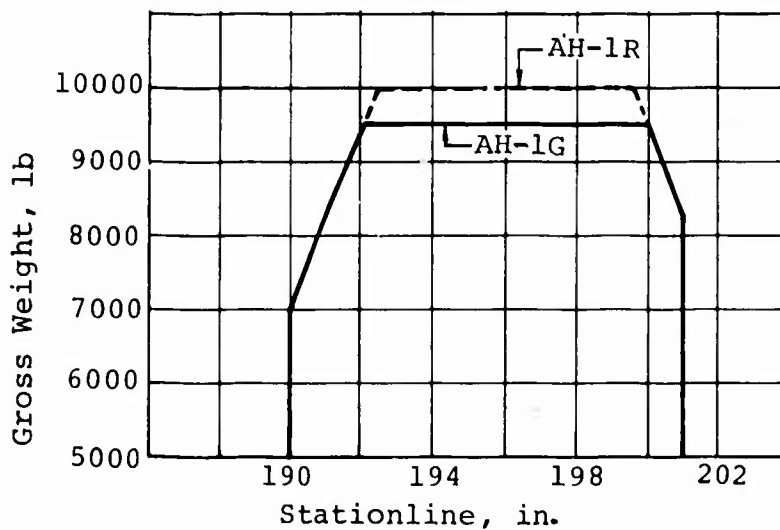


Figure 13. AH-1 loading limits.

TABLE 2. AH-1G/R MAIN ROTOR RPM LIMITS

Power On	
Steady	314 to 324 rpm
Transient	314 to 324 rpm
Power Off	
Steady	294 to 339 rpm
Transient (lower limit)	250 rpm

with this t_c are presented as functions of gross weight in Figure 14. The maximum fuselage rate and attitude limits considered tolerable by a pilot, as presented in Reference 1, are listed in Table 3. The target time for attaining the required high g-level was chosen as three seconds. Times shorter than three seconds resulted in unacceptably high rate/attitude combinations for the helicopter.

The target g-level for low g maneuvers was 0.2g. This value was based upon the time required to complete a simulation of a maneuver at low g-levels, as well as for repeatability purposes.

The roll reversals were initiated by slowly rolling the helicopter to a bank angle of 45 degrees. From this bank angle, a lateral cyclic input was introduced to roll the helicopter in the opposite direction at a peak rate of 60 degrees per second. Upon attainment of the 60-degree-per-second rate, the recovery phase of the maneuver was initiated to return the helicopter to level flight.

Successful autorotation entry was the goal of the engine failure simulation. The rpm decay, fuselage rates and attitude, and other response characteristics were correlated, using Reference 9, so that realistic control limits could be established for successful recovery.

3.2.1 Effect of Center of Gravity

The baseline center of gravity used in this simulation was 196 inches, or neutral cg. The cg range of the AH-1 series varies from 190 inches to 201 inches. Maneuvers were evaluated at these limits, as well as to cg positions of 186 inches and 205 inches, these being points outside the present operational limits.

3.2.1.1 High-G Maneuver (CG Variations)

The maximum flapping peaks recorded during these maneuvers varied as a function of center of gravity. This linear variation was approximately 0.6 degree change in flapping per inch change in cg at the baseline gross weight. At forward cg loadings, the maximum peak was aft flapping during initiation of the maneuver. At aft cg, the peak was forward flapping during the recovery phase. Changes in control input from cyclic only to cyclic plus collective or unsymmetrical (pullout in a constant altitude coordinated turn) did not change the magnitude of the flapping peaks for a particular configuration. These results are presented in Table 4. A typical high-g maneuver is represented by the flight test correlation maneuvers presented in Figures 4, 10 and 11.

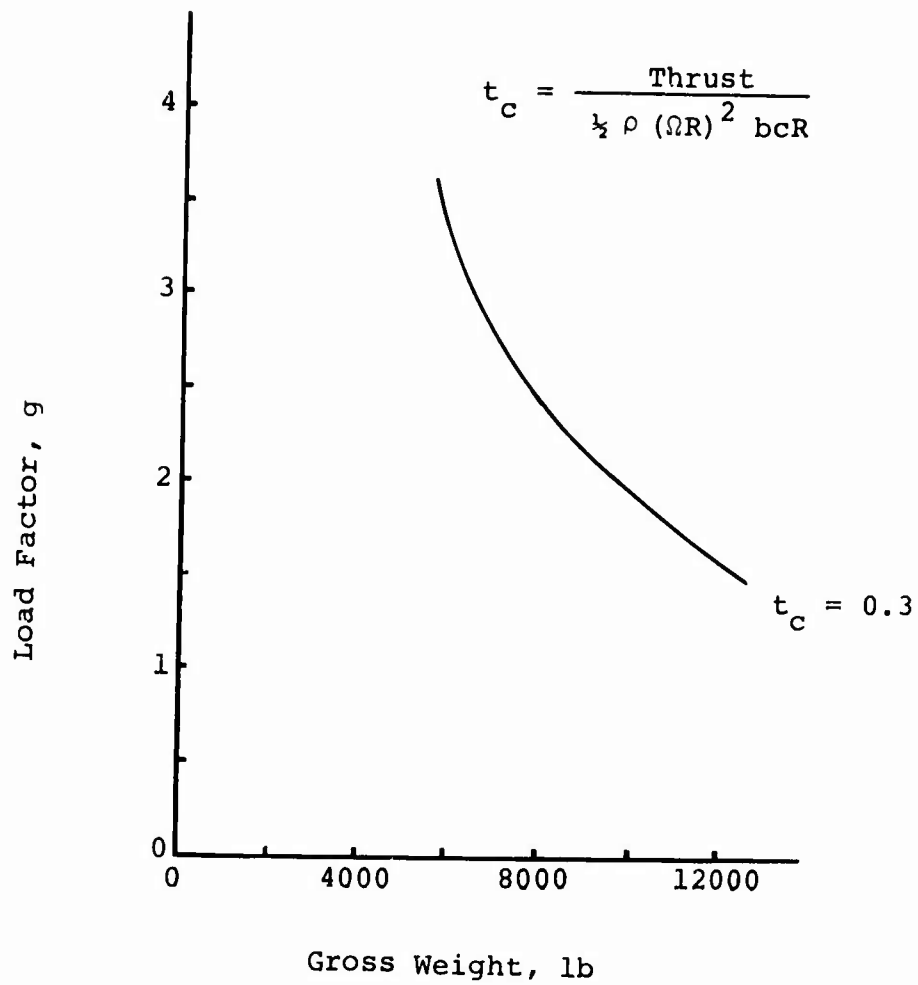


Figure 14. Target load factor variation with gross weight (sea level standard day atmosphere).

TABLE 3. AH-1G/R FUSELAGE RATE AND ATTITUDE LIMITS

Fuselage	Absolute Limits	Combination Limits	
Pitch Angle	±50 degrees	+20 degrees with	-20 degrees with
Pitch Rate	±20 degrees/second	+15 degrees/ second	-10 degrees/ second
Roll Angle	±70 degrees	±55 degrees with	
Roll Rate	±60 degrees/second	±25 degrees/ second	
Yaw Rate	±55 degrees/second (hover) ±15 degrees/second (fwd flt)		

TABLE 4. EFFECT OF CENTER OF GRAVITY ON
AH-1G/R HIGH-G MANEUVERS

Maneuver Number	Control Input	Center of Gravity (in.)	Maximum g Level	Maximum Peak Flapping (deg)	Azimuth of Peak Flapping
10	Cyclic	186	2.4	9.5	Aft
11	Cyclic	190	2.4	7.2	Aft
1	Cyclic	196	2.4	3.6	Aft and Forward
12	Cyclic	201	2.4	6.5	Forward
13	Cyclic	205	2.4	9.0	Forward
14	Cyclic + Collective	186	2.4	10.0	Aft
15	Cyclic + Collective	190	2.4	7.0	Aft
2	Cyclic + Collective	196	2.6	4.0	Aft and Forward
16	Unsymmetrical	186	2.3	9.5	Aft
17	Unsymmetrical	190	2.4	7.5	Aft
3	Unsymmetrical	196	2.4	4.0	Aft and Forward

3.2.1.2 Low-g Maneuvers (CG Variations)

The evaluation of low-g maneuvers indicated that pilot technique can have significant effect on flapping. Flapping levels increased with increasing aft cg loadings for similar pilot control inputs, as would be expected, since aft cg loadings require more forward rotor disc tilt in trimmed flight. However, in the low-g environment, this study revealed that flapping can be influenced more by pilot-related factors than by the physical variables which were evaluated. Due to the reduced main rotor control power, pilot technique and reaction time for entry and recovery from low-g can vary significantly without, in some cases, affecting helicopter rates or attitude significantly. The primary motion the pilot must control is the tendency of the helicopter to roll right as low-g conditions are entered, due mainly to the constant tail rotor thrust. The logical pilot reaction would be a left lateral cyclic input and possibly some change in pedal position. However, the lateral tilt of the rotor plane provides little rolling moment at low g, and if pedal position is changed significantly, a yawing motion can couple with roll. The result may be excessive flapping as the pilot continues to over control in roll and yaw instead of applying aft cyclic to exit the low-g condition.

The effect on flapping of varying control inputs in a maneuver is illustrated in Figure 15. A low-g maneuver was simulated at a gross weight of 8000 pounds and a cg of 190 inches using two slightly different control input techniques to maintain control and produce the desired g-level during the maneuver. Peak flapping of 11 degrees occurred in maneuver A (dashed line), while 8.5 degrees flapping was the maximum in maneuver B (solid line). The 11-degree peak resulted from the large lateral cyclic control input used to stop the right roll rate. A slightly different set of control inputs (maneuver B) reduced the maximum flapping by 2.5 degrees. These differences are primarily due to a small change in pedal input during the maneuver which, because of the strong dihedral stability of the helicopter, resulted in different roll rates and in required corrective control inputs.

Variations of this type in control motion over short periods of time by the pilot made the evaluation of flapping as a function of cg quite difficult. It should again be noted that the target g-level for these maneuvers was 0.2g, which did provide the pilot with some control power. Results for the low-g maneuvers are presented in Table 5.

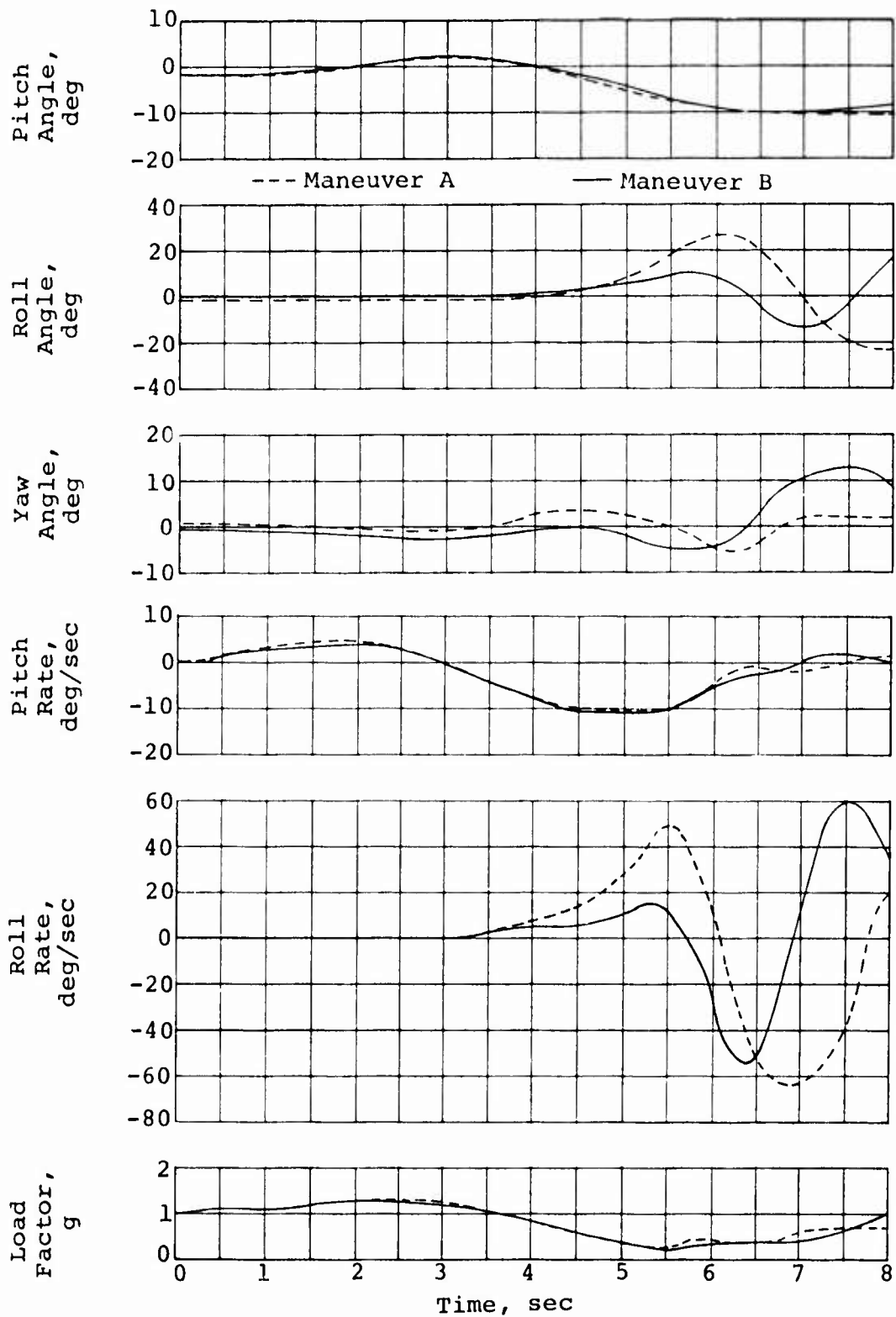


Figure 15. AH-1G/R simulated low-g maneuvers at 120 knots.

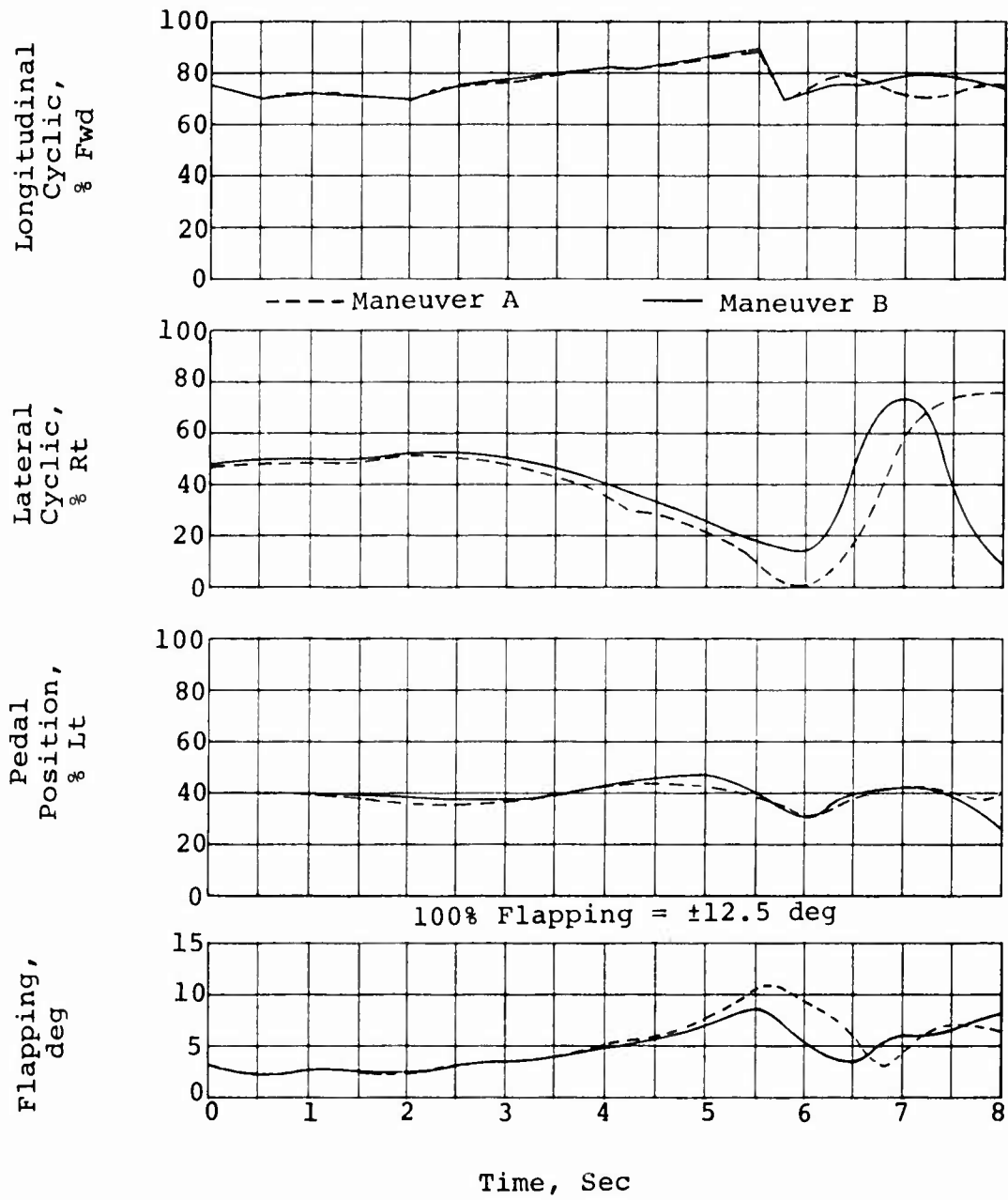


Figure 15. Concluded.

TABLE 5. EFFECT OF CENTER OF GRAVITY ON
AH-1G/R LOW-G MANEUVERS

Maneuver Number	Control Input	Center of Gravity (in.)	Minimum g Level	Maximum Peak Flapping (deg)	Azimuth of Peak Flapping
18	Cyclic	186	0.2	7.0	Forward to Left
19	Cyclic	190	0.2	8.0	Forward to Left
4	Cyclic	196	0.05	8.5	Forward to Left
20	Cyclic	201	0.2	9.0	Forward to Left
21	Cyclic	205	0.2	10.0	Forward to Left
5	Cyclic + Collective	196	-0.55	12.0	Forward
22	Cyclic + Collective	201	-0.55	13.5*	Forward
6	Unsymmetrical	196	0.15	13.5*	Forward
23	Unsymmetrical	201	0.15	13.5*	Forward

*Contacted Flapping Stops by Exceeding ± 12.5 deg

Cyclic plus collective maneuvers resulted in negative load factors for very short periods of time. However, due to the short periods, about 1 second, they were more controllable than cyclic-only low-g maneuvers. Results for these low-g maneuvers are also presented in Table 5. An example of this type maneuver is seen in Figure 4 of the Model 214A flight test correlation maneuver.

Pushovers using unsymmetrical control inputs were initiated by pushing the cyclic stick forward from a banked coordinated turn at a constant altitude. Recovery from this condition required a greater coordination of control inputs than was required for level flight pushovers and, because of the orientation of the helicopter during recovery, this resulted in higher peak flapping levels. Results for these maneuvers are presented in Table 5. For these unsymmetrical maneuvers the flapping stops were contacted.

3.2.1.3 Roll Reversals (CG Variations)

The effect of longitudinal center-of-gravity changes was minor for roll reversals. This is as expected and the results are tabulated in Table 6.

3.2.1.4 Engine Failures (CG Variations)

The maximum flapping peaks increased with shifts to forward cg for engine failures; this is because the trim position of the rotor disc shifts aft with a forward shift in cg. Since recovery is initiated with aft cyclic to slow down and enter autorotation, larger values of aft disc tilt are commanded. An example engine failure at a cg of 190 inches is presented in Figure 16. As was the case for the low-g maneuvers, pilot technique for autorotation entry had a significant effect on flapping. If recovery was delayed for more than 1.5 seconds, the helicopter attitude and rpm decay became excessive at 140 knots, which is approximately the maximum torque condition. These results agreed with flight test data. Recovery from this condition yielded high flapping because of the rapid pilot control inputs which were required. Results for engine failures are presented in Table 7.

3.2.2 Effect on Gross Weight

The baseline gross weight used for this simulation was 8000 pounds. In addition to this baseline, simulations were made with weights of 6000, 10,000, 11,000, and 12,000 pounds according to the configuration matrix (Table 1).

TABLE 6. EFFECT OF CENTER OF GRAVITY ON
AH-1G/R ROLL REVERSALS

Maneuver Number	Direction	Center of Gravity (in.)	Maximum Peak Flapping (deg)	Azimuth Peak Flapping
24	RT	190	8.5	Forward to Left
7	RT	196	8.5	Forward to Left
25	RT	201	9.5	Forward to Left
26	LT	190	8.5	Aft to Right
8	LT	196	9.0	Aft to Right
27	LT	201	8.0	Aft to Right

TABLE 7. EFFECT OF CENTER OF GRAVITY ON
AH-1G/R ENGINE FAILURES

Maneuver Number	Center of Gravity (in.)	Maximum Peak Flapping (deg)	Azimuth of Peak Flapping
28	190	10.0	Aft
9	196	7.5	Aft
29	201	7.0	Aft

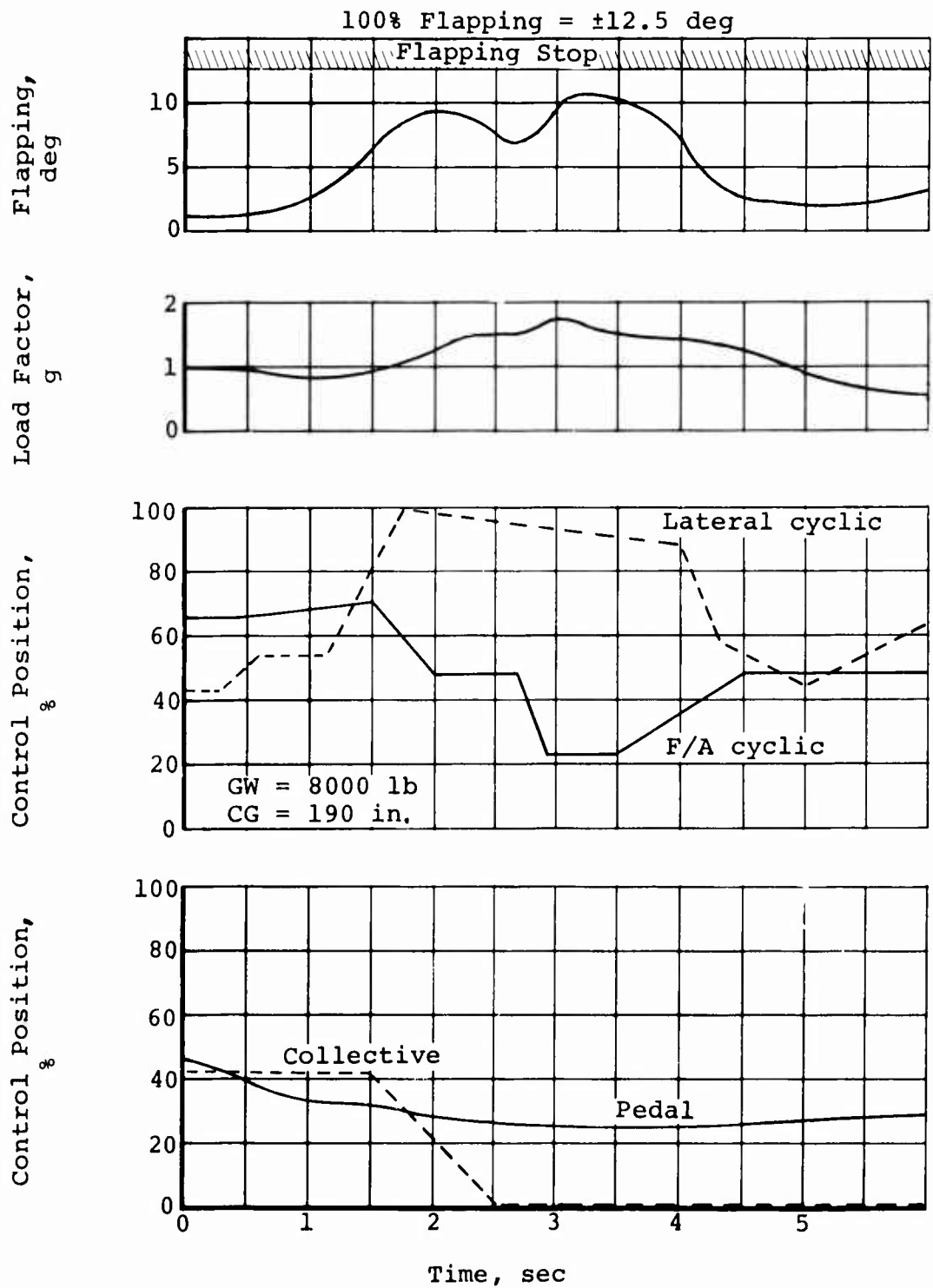


Figure 16. AH-1G/R engine failure and recovery at 140 knots.

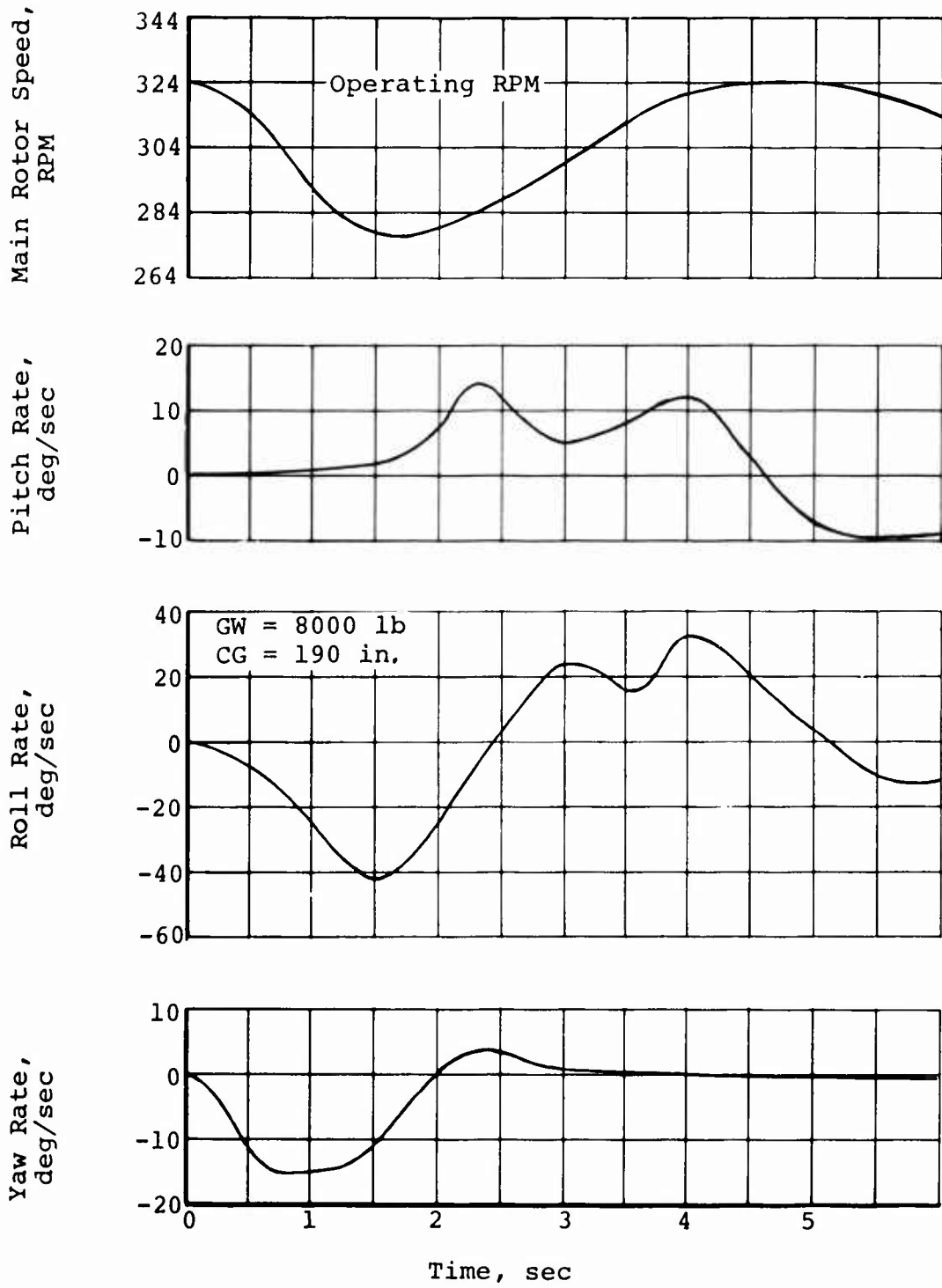


Figure 16. Concluded.

3.2.2.1 High-g Maneuvers (GW Variations)

The maximum flapping increased with increasing g-level. This resulted in higher flapping at low gross weight since, due to the constant maximum blade t_c used for this maneuver, higher g-levels were possible. However, these increases were small when compared with the available margins for allowable flapping. Variations in the three types of control input had little effect on flapping as long as the same g-level was obtained. Results for the high-g maneuvers are presented in Table 8.

3.2.2.2 Low-g Maneuvers (GW Variations)

Peak flapping, as a function of gross weight, did not vary significantly for any of the three particular types of low-g maneuvers. Due to the influence of control inputs, as discussed in Section 3.2.1.2, trends in flapping were not conclusive.

The cyclic-only maneuvers varied through a range of two degrees with no particular trend. These results are presented in Table 9. The cyclic plus collective and unsymmetrical maneuvers yielded flapping levels which were within a degree below to a degree beyond the flapping stop limit of 12.5 degrees. However, no trend with regard to gross weight is clearly discernible. These results are also presented in Table 9.

3.2.2.3 Roll Reversals (GW Variations)

Roll reversal maneuvers evaluating the effects of gross weight variation yielded small changes in peak flapping. These results are shown in Table 10. The effect of gross weight was less pronounced in right roll reversals than in those to the left. This is principally because insufficient right lateral cyclic stick control margin is available at the heavy gross weight to reach the target roll rate of 60 degrees per second as rapidly as desired.

3.2.2.4 Engine Failures (GW Variations)

The variation in gross weight for similar control inputs did not change the flapping peak magnitudes. Variations in power required, which influence engine failures the most, were not significantly different enough at 140 knots to produce a different helicopter response. These data are tabulated in Table 11.

TABLE 8. EFFECT OF GROSS WEIGHT ON
AH-1G/R HIGH-G MANEUVERS

Maneuver Number	Control Input	Gross Weight (lb)	Maximum g Level	Maximum Peak Flapping (deg)	Azimuth of Peak Flapping	Maximum Pitch Rate (deg/sec)
33	Cyclic	6000	2.9	5.2	Aft	27
1	Cyclic	8000	2.4	3.6	Aft	22
32	Cyclic	10000	1.9	3.4	Aft	15
31	Cyclic	11000	1.8	3.3	Aft	13
30	Cyclic	12000	1.6	3.0	Aft	11
2	Cyclic + Collective	8000	2.6	4.0	Aft	22
34	Cyclic + Collective	11000	1.8	3.5	Aft	13
3	Unsymmetrical	8000	2.4	4.0	Aft	22
35	Unsymmetrical	11000	1.8	3.5	Aft	14

TABLE 9. EFFECT OF GROSS WEIGHT ON AH-1G/R
LOW-G MANEUVERS

Maneuver Number	Control Input	Gross Weight (lb)	Minimum g Level	Maximum Peak Flapping (deg)	Azimuth of Peak Flapping
39	Cyclic	6000	0.2	8.0	Forward to Left
4	Cyclic	8000	0.05	8.5	Forward to Left
38	Cyclic	10000	0.25	7.0	Forward to Left
37	Cyclic	11000	0.2	8.0	Forward to Left
36	Cyclic	12000	0.2	9.0	Forward to Left
5	Cyclic + Collective	8000	-0.55	12.0	Forward
40	Cyclic + Collective	11000	-0.5	13.5*	Forward
6	Unsymmetrical	8000	0.15	13.5*	Forward
41	Unsymmetrical	11000	0.2	11.5	Forward

*Contacted Flapping Stops by Exceeding ± 12.5 deg

TABLE 10. EFFECT OF GROSS WEIGHT ON
AH-1G/R ROLL REVERSALS

Maneuver Number	Direction	Gross Weight (lb)	Maximum Peak Flapping (deg)	Azimuth Peak Flapping	Maximum Roll Rate (deg/sec)
7	RT	8000	8.5	Forward to Left	60
42	RT	10000	8.0	Forward to Left	60
8	LT	8000	9.0	Aft to Right	61
43	LT	10000	7.5	Aft to Right	56

TABLE 11. EFFECT OF GROSS WEIGHT ON
AH-1G/R ENGINE FAILURES

Maneuver Number	Gross Weight (lb)	Maximum Peak Flapping (deg)	Azimuth of Peak Flapping
9	8000	7.5	Aft
44	11000	7.5	Aft

3.2.3 Effect of Rotor Speed

The baseline rotor speed was the normal operating main rotor rpm of 324 revolutions per minute . The variations of this parameter which were investigated were 339, 294, and 274 rpm (see Table 2 for rpm limits).

3.2.3.1 High-g Maneuvers (RPM Variation)

The variation of main rotor rpm for high-g maneuvers did not produce significant changes in flapping for the constant blade t_c of 0.3. The total variation among flapping peaks was 1.5 degrees for the three types of control input which were investigated. These data are presented in Table 12. The effects of stall at lower rpm did not have a significant effect upon flapping since the initial blade t_c was kept constant at 0.3. For that t_c , stall was not approached until after initiation of the high-g maneuver. These stall characteristics, while modeled mathematically, should be interpreted as a tendency toward increased flapping, but the absolute value of flapping obtained may be questionable.

3.2.3.2 Low-g Maneuvers (RPM Variations)

Low-g maneuvers were not significantly affected by variations in rpm. The cyclic-only maneuvers were all within 2 degrees flapping of one another. This difference in flapping at low-g levels is within the variation that can be expected due to the low available control power and the resulting variation in pilot control input. Cyclic plus collective maneuvers varied in flapping by less than one degree for almost identical control inputs, and unsymmetrical maneuvers varied by 1.5 degrees. Results from these low-g maneuvers are presented in Table 13.

3.2.3.3 Roll Reversals (RPM Variations)

The effects of rotor rpm were minimal on roll reversals. Variations in flapping among the maneuvers evaluated were within a degree or less for all maneuvers. This variation is well within the influence of effects on flapping due to the differences in control motion required in meeting the target roll attitude and rate parameters. The data from these maneuvers are compared in Table 14.

TABLE 12. EFFECT OF MAIN ROTOR RPM ON AH-1G/R
HIGH-G MANEUVERS

Maneuver Number	Control Input	RPM	Maximum g Level	Maximum Peak Flapping (deg)	Azimuth of Peak Flapping
45	Cyclic	339	2.6	4.5	Aft
1	Cyclic	324	2.4	3.6	Aft
46	Cyclic	294	2.0	3.6	Aft
47	Cyclic	274	1.75	4.8	Aft
2	Cyclic + Collective	324	2.6	4.0	Aft
48	Cyclic + Collective	294	2.0	3.5	Aft
3	Unsymmetrical	324	2.4	4.0	Aft
49	Unsymmetrical	294	2.4	5.0	Aft

TABLE 13. EFFECT OF MAIN ROTOR RPM ON AH-1G/R
LOW-G MANEUVERS

Maneuver Number	Control Input	RPM	Minimum g Level	Maximum Peak Flapping (deg)	Azimuth Peak Flapping
50	Cyclic	339	0.25	10.5	Forward to Left
4	Cyclic	324	0.05	8.5	Forward to Left
51	Cyclic	294	0.2	8.5	Forward to Left
52	Cyclic	274	0.2	8.5	Forward to Left
5	Cyclic + Collective	324	-0.55	12.0	Forward
53	Cyclic + Collective	294	-0.6	11.5	Forward
6	Unsymmetrical	324	0.15	13.5	Forward
54	Unsymmetrical	294	0.25	11.0	Forward

TABLE 14. EFFECT OF MAIN ROTOR RPM ON
AH-1G/R ROLL REVERSALS

Maneuver Number	Direction	RPM	Maximum Peak Flapping (deg)	Azimuth of Peak Flapping	Maximum Roll Rate (deg/sec)
7	RT	324	8.5	Forward to Left	60
55	RT	294	9.0	Forward to Left	60
56	RT	274	9.0	Forward to Left	60
3	LT	324	9.0	Aft to Right	60
57	LT	294	8.0	Aft to Right	60
58	LT	274	8.0	Aft to Right	60

3.2.4 Effect of Power Required

Maneuvers were simulated for the initial flight conditions of maximum power climb, level flight, and autorotation to evaluate effects on rotor flapping of power required at 120 knots. The maximum power climbs were made using a main rotor power of 1160 shp. This power level is available for five minutes to the main rotor using the AH-1G. The power required for level flight at 120 knots is about 730 horsepower for the baseline condition.

3.2.4.1 High-g Maneuvers (Power Variations)

The effect of both autorotation and climb was to increase peak flapping from that experienced when maneuvers were entered from level flight. Using cyclic control inputs only, the flapping peaks in the maximum power climb and the autorotation were 2.0 degrees and 1.5 degrees respectively, above the flapping peak of 3.5 degrees for the high-g maneuver entered from level flight. However, these flight conditions using cyclic-only control movements did not yield large magnitudes of flapping. For cyclic-only maneuvers, it was hard to keep the main rotor from overspeeding; therefore, the simultaneous movement of cyclic and collective is considered a more realistic input of control motion. Table 15 compares data from these maneuvers.

TABLE 15. EFFECT OF POWER ON AH-1G/R HIGH-G MANEUVERS

Maneuver Number	Control Input	Flight Condition	Maximum g Level	Maximum Peak Flapping (deg)	Azimuth of Peak Flapping
59	Cyclic	Climb	2.4	5.5	Aft
1	Cyclic	Level	2.4	3.6	Aft
60	Cyclic	Autorotation	2.2	5.0	Aft
2	Cyclic + Collective	Level	2.6	4.0	Aft
61	Cyclic + Collective	Autorotation	2.5	11.0	Aft
3	Unsymmetrical	Level	2.4	4.0	Aft
62	Unsymmetrical	Autorotation	2.4	8.5	Aft

During the investigation of cyclic plus collective control inputs in autorotation, it was demonstrated that peak flapping is related to both the rate and magnitude of the longitudinal cyclic control inputs. At the baseline gross weight and center of gravity, a pull-up to over 2.5g's was simulated with two different longitudinal control input methods. In the first, a cyclic input of 17 percent at a rate of 11.3 percent/second was used to generate a flapping peak of 6 degrees occurring at 3.8 seconds after the start of control movements. The second maneuver used a 30-percent input at 120 percent/second with a flapping peak of 11 degrees to obtain the same g level 2 seconds after the start of control movement. The large, abrupt control input called for large fuselage acceleration. When cyclic inputs are applied so quickly, the fuselage cannot respond as fast as the rotor and the rotor will flap approximately the same as the swashplate motion. For this case, the change in flapping due to the cyclic input was almost equal to the magnitude of the swashplate input. With the smaller, slower input, the fuselage started to rotate before the cyclic input was complete, which tended to relieve the commanded flapping.

These results illustrate the importance of using smooth, coordinated control inputs to maneuver the helicopter if flapping is to be held to a minimum.

The maneuvers using unsymmetrical control inputs required similar inputs to the cyclic plus collective maneuvers. The results, especially in autorotation, were similar.

3.2.4.2 Low-g Maneuvers (Power Variations)

Low-g maneuvers were simulated for cyclic-only control inputs. Pushovers from climb resulted in about a 3-degree increase in peak flapping when compared to level flight; whereas, the autorotation pushover peaks were about 3 degrees less. Peak flapping occurred in the low-g portion of all three maneuvers and corresponded to the left lateral cyclic inputs supplied to arrest the right roll inherent in the low-g maneuver. The differences in peak flapping were the result of differences in trimmed flight flapping, minimum g-level reached, and lateral cyclic input to correct the right roll tendency of the helicopter under low-g conditions. The effect of initial power on flapping in low-g maneuvers is given in Table 16.

3.2.4.3 Roll Reversals (Power Variations)

Left and right roll reversals initiated from level flight resulted in flapping peaks which were within 0.5 degree of one another. Results of these maneuvers are tabulated in Table 17.

TABLE 16. EFFECT OF POWER ON AH-1G/R LOW-G MANEUVERS

Maneuver Number	Control Input	Flight Condition	Minimum g Level	Maximum Peak Flapping (deg)	Azimuth Peak Flapping
63	Cyclic	Climb	0.15	11.0	Forward to Left
4	Cyclic	Level	0.05	8.5	Forward to Left
64	Cyclic	Autorotation	0.2	5.5	Forward to Left

TABLE 17. EFFECT OF POWER ON AH-1G/R ROLL REVERSALS

Maneuver Number	Direction	Flight Condition	Maximum Peak Flapping (deg)	Azimuth of Peak Flapping	Maximum Roll Rate (deg/sec)
65	RT	Climb	10.5	Forward to Left	62
7	RT	Level	8.5	Forward to Left	60
66	RT	Autorotation	11.0	Forward to Left	57
67	LT	Climb	8.5	Aft to Right	58
8	LT	Level	9.0	Aft to Right	60
68	LT	Autorotation	7.5	Aft to Right	60

In a maximum power climb, the right roll reversal yielded a larger flapping peak than the left roll reversal.

In simulating the maximum power climbs, the same control input technique was maintained wherever possible. Some of the difference in maximum flapping between the two climb maneuvers can be attributed to tail rotor effects. This results from the large amount of tail rotor thrust required in a trimmed climb when compared with level flight. During recovery from right roll reversals, the tail rotor thrust opposes recovery, thereby requiring more lateral cyclic. However, it must again be emphasized that roll reversals are sensitive to lateral inputs (see discussion in Section 2.2.1).

In autorotation, the left and right roll reversals yielded flapping peaks which were different from each other by 3.5 degrees. One reason for this difference results from the lateral cyclic trim position in autorotation. In the attainment of the target roll angles and rates, the maneuvers required different techniques which do not make the maneuvers comparable. The peak flapping of 11 degrees for the right roll reversal was obtained in the initialization of the 60-degree-per-second roll rate, and the ± 7.5 degrees of the left roll reversal was obtained during recovery from the 60-degree-per-second roll rate.

3.2.4.4 Engine Failures

Simulation of engine failures was attempted at 140 knots with a delay time of 1.5 seconds for control inputs. The flapping peak for an engine failure from level flight was 7.5 degrees. These data are presented in Table 18. An engine failure was attempted in a shallow climb at 140 knots; however, the use of a control delay resulted in a loss of control of the helicopter due to excessive fuselage attitudes and rates. This compares closely with the trends measured in flight test which are presented in Reference 9. To obtain adequate time for recovery delay, a failure at 120 knots was attempted and the flapping peak during this maneuver was computed at 8.5 degrees. The flapping peak for level flight recovery at 120 knots was approximately 7.0 degrees with a longer available recovery delay time possibly due to the reduced horsepower requirements.

TABLE 18. EFFECT OF POWER ON AH-1G/R ENGINE FAILURES

Maneuver Number	Flight Condition	Maximum Peak Flapping (deg)	Azimuth of Peak Flapping
69	Climb*	8.5	Aft
9	Level	7.5	Aft
9	Level*	7.0	Aft

*Evaluated at 120 knots.

3.2.5 Configuration Effects

The configuration change which was evaluated resulted in a change from the baseline case of the AH-1 with four wing rocket pods to the AH-1 with clean wings. No significant changes were noticed in flapping for any of the envelope expansion maneuvers. The only results of importance were the slightly reduced stick travel requirements during roll reversals due to roll inertia reduction and the potentially improved delay time for recovery from engine failure due to the lower power requirements for the reduced drag of the configuration. These effects, however, were not evaluated since flapping was not significantly affected and flight test evaluations are available (Reference 9).

3.3 RESULTS OF ENVELOPE LIMIT STUDIES

Based on these simulations, the most critical envelope for the AH-1 helicopter appears to be the low-g load factor restriction. During low-g maneuvers, high flapping could result for almost any combination of other AH-1 operational envelope parameter variations if instinctive pilot inputs are used. Flapping stop contact was predicted for some simulated conditions.

The next most sensitive envelope is center-of-gravity location. Center-of-gravity extremes can increase flapping in maneuvers in either initiation or recovery phases. While center-of-gravity extremes do show high flapping peaks, no stop contact was predicted based on cg location alone if the low-g flight regime is avoided.

The gross weight, main rotor rpm, and vehicle configuration affected flapping to a lesser degree. Engine power was most critical in engine failures due to the resultant rapid fuselage excursions and rotor rpm decay rates that required large abrupt control inputs for recovery.

Pilot technique was very important in controlling flapping. Large, rapid control inputs resulted in higher flapping than that obtained with more gradual control inputs for the same type of maneuvers.

As stated in Reference 1, the stability characteristics of the helicopter (aerodynamic, geometric, inertial, and control system) have a strong influence on main rotor flapping. Thus, if these simulations were performed for a different helicopter, the results may be different. However, the results presented here are representative of helicopters with two-bladed teetering rotors.

4. METHODS OF EXTENDING OPERATIONAL ENVELOPES

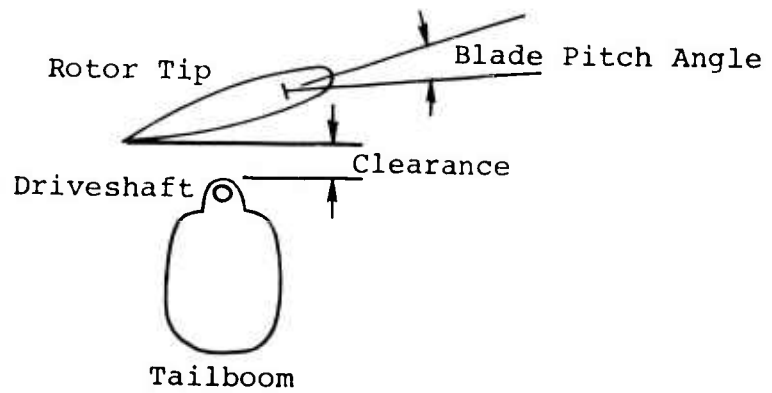
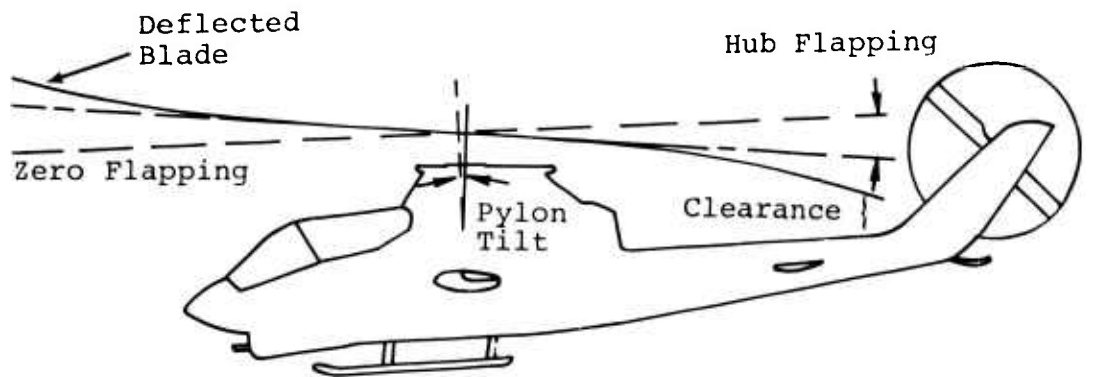
From these studies and those of Reference 1, several basic causes of high flapping have been identified. The purpose of this section is to investigate promising methods to reduce flapping or to increase safety margins in cases of high flapping.

Three broad categories of study are presented. First, the proposal to eliminate flapping stop contact by increasing allowable flapping before the flapping stops are contacted. Second, to provide control inputs that reduce flapping before stop contact. These inputs may be directly to the rotor or to the pilot. Third is the approach to reduce the consequences of flapping stop contact on the mast and rotor assemblies.

4.1 INCREASED HUB FLAPPING CLEARANCE

Main rotor blade flapping stops are required to ensure adequate rotor-to-fuselage clearance under static or low rotor speed conditions which, of course, are encountered every time the rotor is started or stopped. At very low rotor speeds, aerodynamic control of the rotor is difficult and, consequently, flapping stops provide the only means of ensuring fuselage/blade clearance. The control at low RPM is further reduced in high winds. For Bell Helicopter Textron helicopters, tailboom clearance is usually the design limit. As shown in Figure 17, the effects of blade flexibility, pylon deflection, and the geometric pitch (including twist) of the blade must be considered in determining the proper flapping stop location.

At normal rotor operating speed, the pilot may control flapping with the cyclic controls to ensure adequate rotor-to-fuselage clearance. If the rotor is also producing thrust, as in flight, the coning of the blades provides additional clearance. Under flight conditions within the operational envelopes of the helicopter, the flapping stops will not be contacted and could possibly be eliminated. Centrifugally operated flapping stops could be used to provide adequate fuselage clearance for rotor starts and stops, and provide an extended flapping envelope at rotor speeds for normal flight operation. However, some conditions make the use of flapping stops desirable even at normal operating rotor speeds. In slope landings, for example, contact with the flapping stops as the helicopter settles provides a warning that the slope is too steep for a safe landing. With increased flapping clearance, this warning would not occur until the helicopter had settled further and the possibility exists that accidents due to landing on excessive slopes could occur.



(Cross-sectional
View From Rear)

Figure 17. Blade to fuselage clearance.

In general, conditions which presently create potential flapping stop contact will become potential fuselage strikes. Therefore, increasing the hub flapping clearance has only limited value.

4.2 METHODS TO REDUCE FLAPPING USING FLIGHT CONTROLS

Rotor flapping is basically an indicator of the amount of angular acceleration of the fuselage commanded by the pilot, aerodynamic, or mechanical signals. Several methods are available to reduce the magnitude of flapping through passive or active control inputs or by modification of the control system to restrict the pilot's control inputs.

4.2.1 Control Rate Limiters

Reference 1 reported that one factor that can produce high flapping is the use of large, abrupt control inputs. Since current helicopters provide hydraulically boosted control systems, a pilot can move the controls with little inherent control force up to the rate limit of the hydraulic actuator that moves the swashplate. Hydraulic actuators normally can travel from one extreme position to the other (a full throw of the actuator) in less than one second (100 percent per second).

One approach to restrict pilot control input is to limit the rate at which he can move the controls. This would assure that abrupt control movements would be impossible. To determine the pure rate restrictions required to reduce flapping, the AH-1G/R simulations of Section 3 provide some guidelines. Extreme flapping in a pullup maneuver was generated using a 60-percent per second cyclic input combined with a 40-percent per second collective input. This indicates that reducing control rate limits to one-half their present values may still allow extreme flapping. Control rate restrictions of this magnitude would probably degrade the handling qualities of the helicopter, since the combination of high rates with small motions are felt to be typical in helicopter operation.

Design specifications do not require a minimum or maximum rate of control movement for satisfactory handling qualities. These specifications are written in terms of minimum magnitudes of helicopter response to a given pilot input.

Bell Helicopter Textron experience has shown that controls that are rate limited to a full throw in approximately three seconds will increase pilot workload to an unsatisfactory level; control systems that have been capable of a full throw in one second have been satisfactory. To determine where between these points the rate restriction would become objectionable, an

evaluation of acceptable rate restrictions would have to be conducted based on pilot opinion under actual mission conditions. Flight testing would be required to determine if restriction of pilot control input is a suitable method to alleviate excessive flapping. If tests were to prove this concept feasible, the rate of control movement could be governed by restrictions in hydraulic actuator flow rates or by modification of force feel systems which might be currently installed.

4.2.2 Force Feel Limiters

An approach to restricting the pilot from applying large, abrupt control inputs is to incorporate a force feel system to resist pilot control inputs. The basic system to be added to the existing control system of the subject helicopter is shown in Figure 18.

The tachometer measures the rate of control stick motions and converts it into an electrical signal. This signal is then integrated to obtain stick displacement from the initial stick position. The product of displacement and rate multiplied by suitable gains are used to generate a DC signal which is amplified and applied to the AC motor.

This causes a resistance to stick motion which will increase the control force required to move the control as shown in Figure 19. Large stick displacements can be made slowly, and small stick displacements can be made rapidly with very little increase in control force felt by the pilot. As both stick rate and displacement increase, the resistance to control increases. This would provide a positive warning to the pilot to avoid large erratic control inputs.

As shown in Figure 18, the force feel limiter would be added to the existing cyclic control system and would be independent of the present magnetic brake force feel system. The same type of device can also be added to the collective controls. This allows the limiter to be active even when the pilot has disengaged the standard force feel system. The limiter is also a fail-passive device requiring no redundancy. In the event a spurious signal is generated, the AC motor will not move due to the DC voltage applied. In case of failure, the pilot would feel a strong control force when he attempted to move the control which could be overcome by slip clutch or shear pin to allow overriding of this force. A circuit breaker would be supplied to disconnect the system in case of malfunction.

The relation between force and control rates and displacements of this device would be best determined through flight tests in which pilot opinion would be used to determine the system characteristics that could best allow control freedom for normal flight but would restrict the pilot from making large, abrupt control inputs.

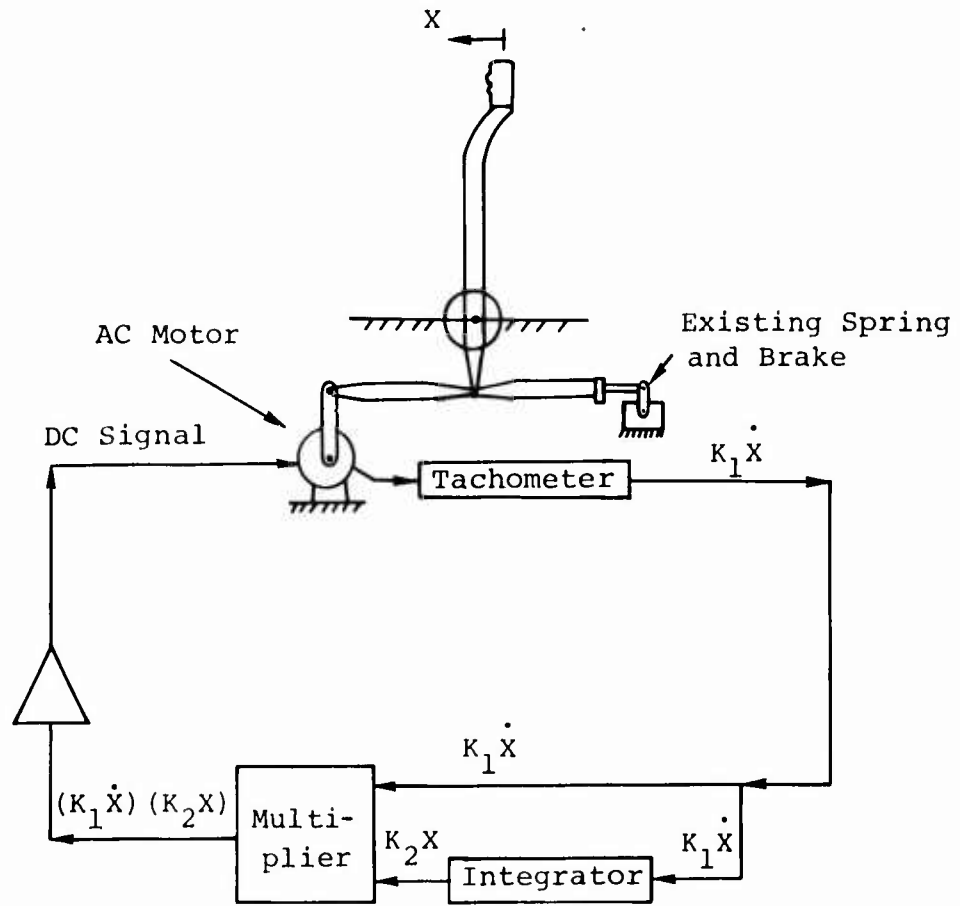


Figure 18. Modified force feel system.

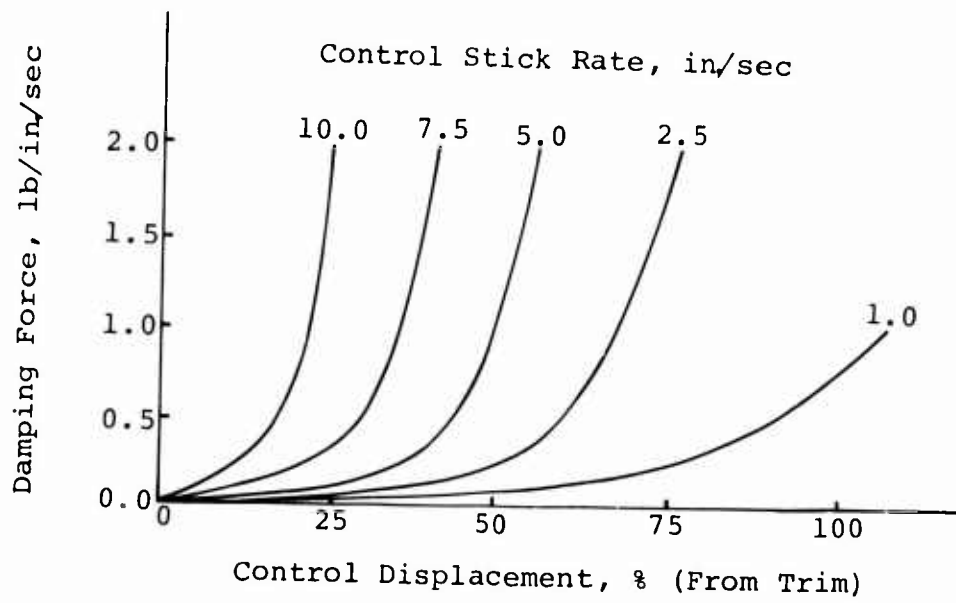
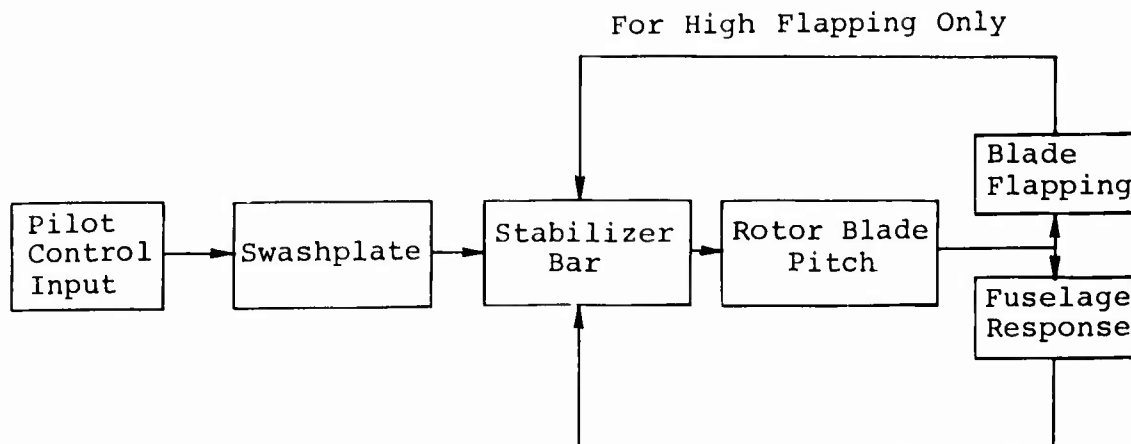


Figure 19. Control damping force variation with control motion.

4.2.3 Active Flapping Controller

Another device which could be used to avoid excessive flapping is one that would detect high flapping and automatically introduce control inputs to reduce the flapping. An early example of this type of device was used on Bell Model 47 helicopters. The control system on this helicopter could be represented as:



The pilot controls move the swashplate, which commands stabilizer bar motion. The stabilizer bar, which also responds to fuselage angular rates, then changes rotor blade pitch in response to both pilot input and fuselage motions. This blade pitch produces a desired fuselage response and a resultant blade flapping. In the Model 47, a cable was attached between the rotor blade and the stabilizer bar such that when blade flapping exceeded a predetermined magnitude, the stabilizer bar was forced to command a blade pitch change that would reduce flapping. The primary purpose of this device was to prevent tailboom strikes by the rotor during hard landings.

In order to analyze the characteristics of this type of system, an electronic flapping controller incorporated in an aircraft equipped with an electro-hydraulic stability and control augmentation system (SCAS) was examined. This provided for determination of basic system requirements in terms of component transfer functions which may then be supplied by either electrical or mechanical devices.

The principal of the flapping controller system is to detect rotor flapping and predict its value during the next half revolution. If the predicted flapping is above a specified level, a cyclic input is supplied through the SCAS actuator

in a direction to reduce flapping. In order to examine the system requirements, the flapping controller was incorporated into the hybrid version of C81. Hybrid computer equipment limitations allowed monitoring of only the longitudinal component of flapping during this simulation; therefore, only longitudinal high flapping maneuvers were examined. A block diagram of the flapping controller is presented in Figure 20.

In the hybrid simulation, the hub flapping is sampled twice per revolution, when the blades pass above the nose and tail-boom of the helicopter. The flapping one-half of a revolution ahead is predicted by adding the current value of flapping to the change in flapping over the preceding one-half revolution. When this prediction is above a specified threshold value, a signal is transmitted to the SCAS actuator commanding a control input to reduce flapping. With a single SCAS actuator, this signal is simply added to the normal SCAS commands. Figure 21 illustrates a pull-up maneuver for an AH-1G/R helicopter and compares flapping for the basic helicopter (SCAS ON) with the same maneuver using the flapping controller. The same pilot control inputs were used in both maneuvers. For this case, the specified flapping threshold which activated the controller was 8 degrees.

While the SCAS actuator reached its stop during the initial portion of the maneuver, the flapping controller drove it there faster than SCAS alone with a resultant slight reduction in flapping. The maximum actuator rate during these maneuvers is a full throw in one quarter of a second. This corresponds to a swashplate actuator rate of a full throw in one second. The flapping reduction in the recovery phase of the maneuver is more significant. The SCAS actuator was not against its stop and the flapping reduction signals were implemented completely. It is during this phase of most maneuvers (when fuselage rates must be reduced) that the flapping controller is most effective.

Incorporation of this device on actual aircraft would involve more information than required for the hybrid C81 simulation. Since flapping can peak at any azimuth, the flapping detection device must determine the azimuth at which peak flapping occurs. The commanded SCAS control input must then be phased properly with a combination of longitudinal and lateral cyclic inputs as required.

The only situation foreseen where the command to change blade pitch in order to reduce flapping may actually increase flapping is when the flapping is down aft due to severe retreating blade stall. In this case, the proper corrective action is reduction of collective pitch rather than application of forward cyclic. A forward cyclic command would increase the pitch of the retreating blades which further aggravates the

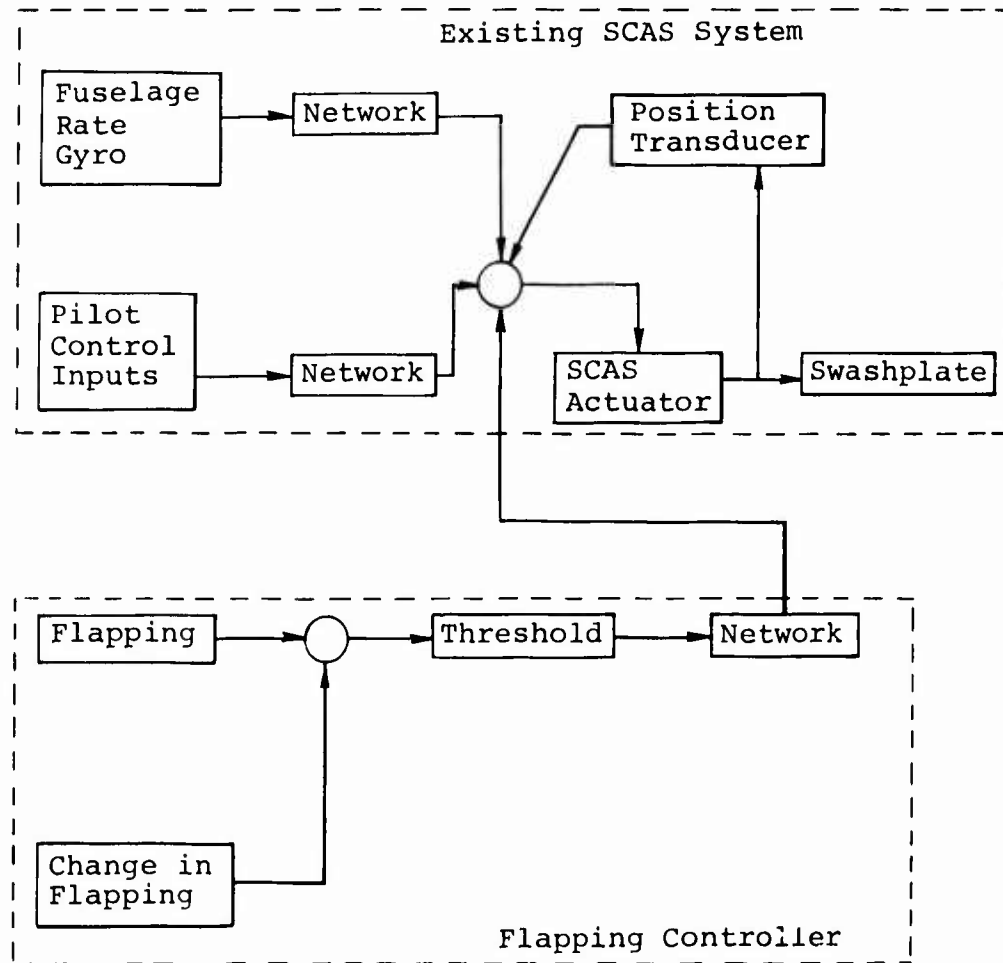


Figure 20. Block diagram of the flapping controller.

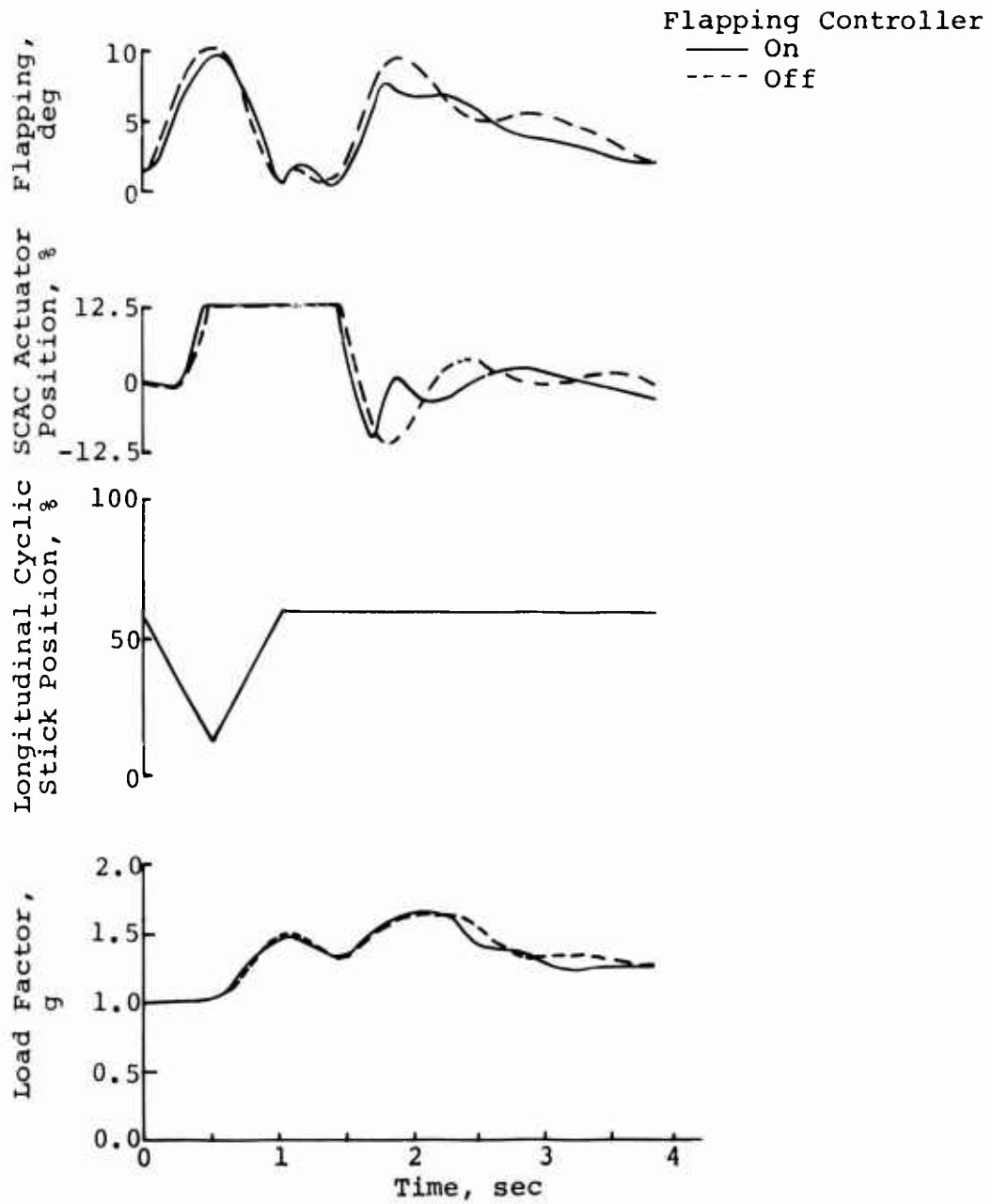


Figure 21. Effect of a flapping controller in a pull-up maneuver.

stall condition. Simulation of this condition was not attempted since the flapping prediction by the hybrid C81 in conditions of severe stall is uncertain. Flight testing of this condition would be required to determine if this phenomenon would present a serious problem to this concept.

4.2.4 Hub Moment Restraint

As reported in Reference 1, the addition of hub restraint to a two-bladed teetering rotor helicopter provided a reduction in flapping for all maneuvers that were investigated. The most significant reduction was in low-g maneuvers.

Hub springs have been tested by BHT on several two-bladed helicopters. From this experience, the application of hub restraint is believed to be feasible within the design guidelines presented here. The magnitude of hub restraint that can be added to existing teetering rotor helicopters is a trade-off between several factors. To provide maximum flapping reduction in maneuvers, the spring rate should be as high as possible. The maximum value of this rate will be limited by a number of factors such as the size of the spring, its effect on the fatigue life of rotor system components, vibration isolation capability, and possibly rotor stability. The most critical of these is usually the effect on fatigue life.

The additional moment on the rotor mast due to the hub restraint must be reacted by hub and blade structure as well as the mast. The fatigue life of these components is strongly affected by maneuvers that produce moderate levels of flapping. While the addition of hub restraint will reduce this flapping, the additional loads due to the spring must not cause the present endurance limit of any component to be exceeded. The fatigue consideration under conditions of moderate flapping will generally limit the maximum permissible spring rate.

Another factor that may limit the maximum spring rate is the effect the spring may have on the vibration isolation capability of the pylon. For teetering rotor helicopters, the pylon spring rate, damping, and geometry have been tailored to isolate a 2/rev shear load at the teetering pin. The hub restraint will add a 2/rev moment to the excitation of the pylon. If the spring rate is high enough, this 2/rev moment may require changes in the isolation system. For the AH-1 and UH-1 series helicopters, the maximum value of spring rate is expected to be the result of fatigue considerations rather than vibration isolation problems.

The stability of the rotor and pylon system may be reduced if a large hub restraint is used; however, the magnitude of spring rate required to cause stability problems is normally well above the limit due to other factors, as indicated by previous analyses.

Within the boundaries specified by the design conditions, a hub restraint of approximately 150 to 200 foot-pounds/degree/blade is felt to be acceptable for the AH-1 and UH-1 series helicopters. With this amount of hub restraint, the hovering control power and damping will be increased by about 15 to 20 percent, which will enhance the low-speed handling qualities.

Since the hub restraint at low to moderate flapping angles may be limited by fatigue considerations, a nonlinear hub spring is proposed to provide a higher level of hub restraint under conditions of high flapping. This additional control power due to the nonlinearity will tend to reduce flapping even more than with a linear spring. The general characteristics of a nonlinear hub spring design are given in Figure 22.

Several design techniques are available to generate this nonlinear type of curve. A promising method to accomplish this is shown in Figure 23. Rubber is attached to brackets that connect to the original hub. (The rubber may be attached directly to the mast instead of being attached with brackets.) As the rotor flaps, the rubber is compressed and will provide a moment on the mast. When properly designed, this moment will be linear for low values of flapping and, as the rubber is compressed to higher strain levels, the moment will increase nonlinearly as the compressed rubber stiffens. At extreme flapping levels, the rubber will compress fully, preventing metal-to-metal contact between the mast and hub. Additionally, the rubber distributes the hub contact load over a larger area on the mast which will reduce the mast stress level for extreme flapping conditions.

In order to evaluate the effect of a nonlinear hub spring on flapping in extreme maneuvers, a nonlinear hub spring was used with the AH-1G/R simulation model discussed in Section 3 of this report. A low-g pushover, using forward cyclic stick along with a drop in collective, was performed with the basic AH-1G/R and then repeated with the inclusion of a nonlinear hub spring. The hub spring characteristics are presented in Figure 24 and the maneuver comparison is presented in Figure 25.

The same longitudinal cyclic and collective pilot inputs were used for both cases. The plotted control positions include the effect of SCAS inputs which change the recovery portion of the maneuver slightly. The flapping reduction due to the nonlinear hub spring is seen to be more than 2 degrees for this maneuver.

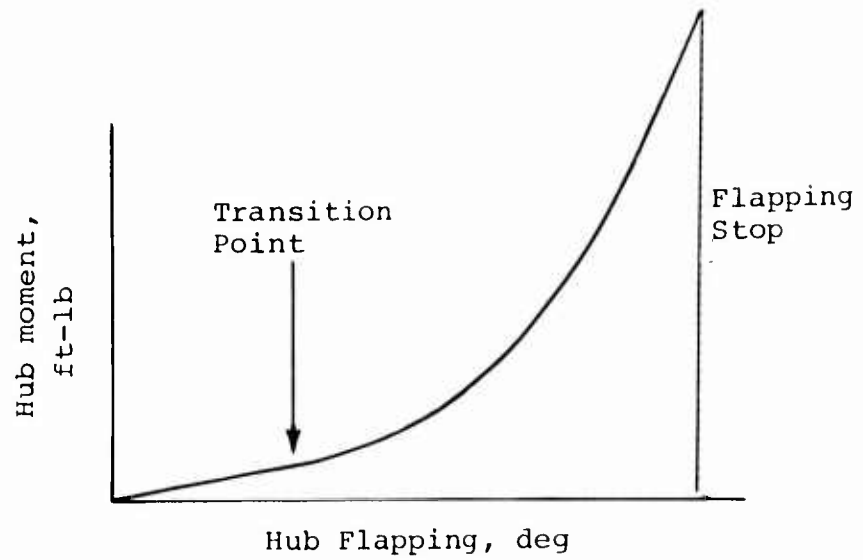


Figure 22. Nonlinear hub spring characteristics.

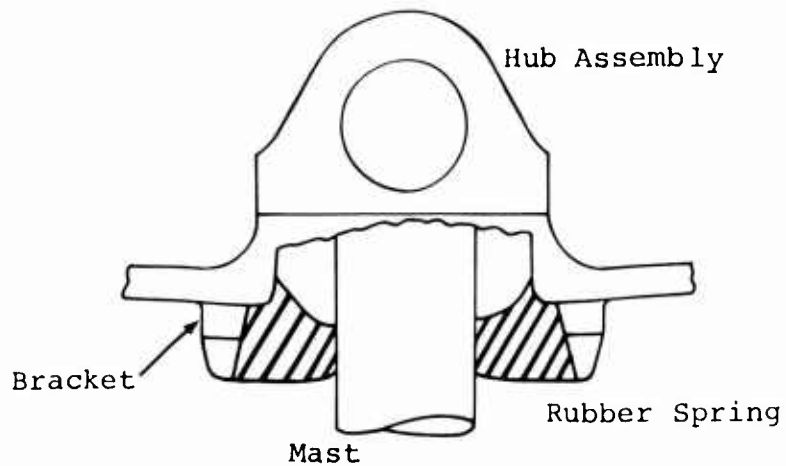


Figure 23. Nonlinear hub spring design.

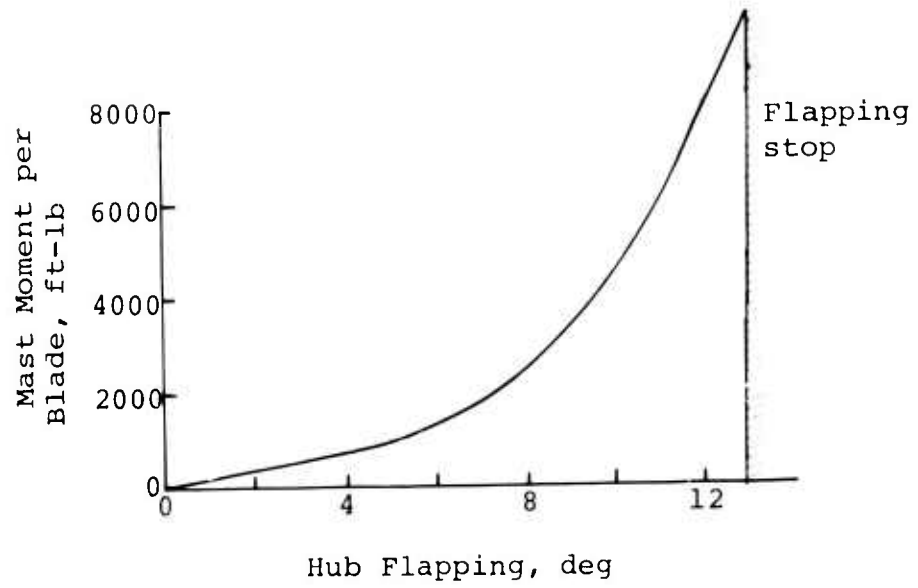


Figure 24. Nonlinear hub spring for AH-1G/R simulation.

AH-1G/R
 GW = 8000 lb
 CG = 196.0 in.
 Entry Airspeed = 120 Kt

— Nonlinear Hub spring
 - - - Basic Ship

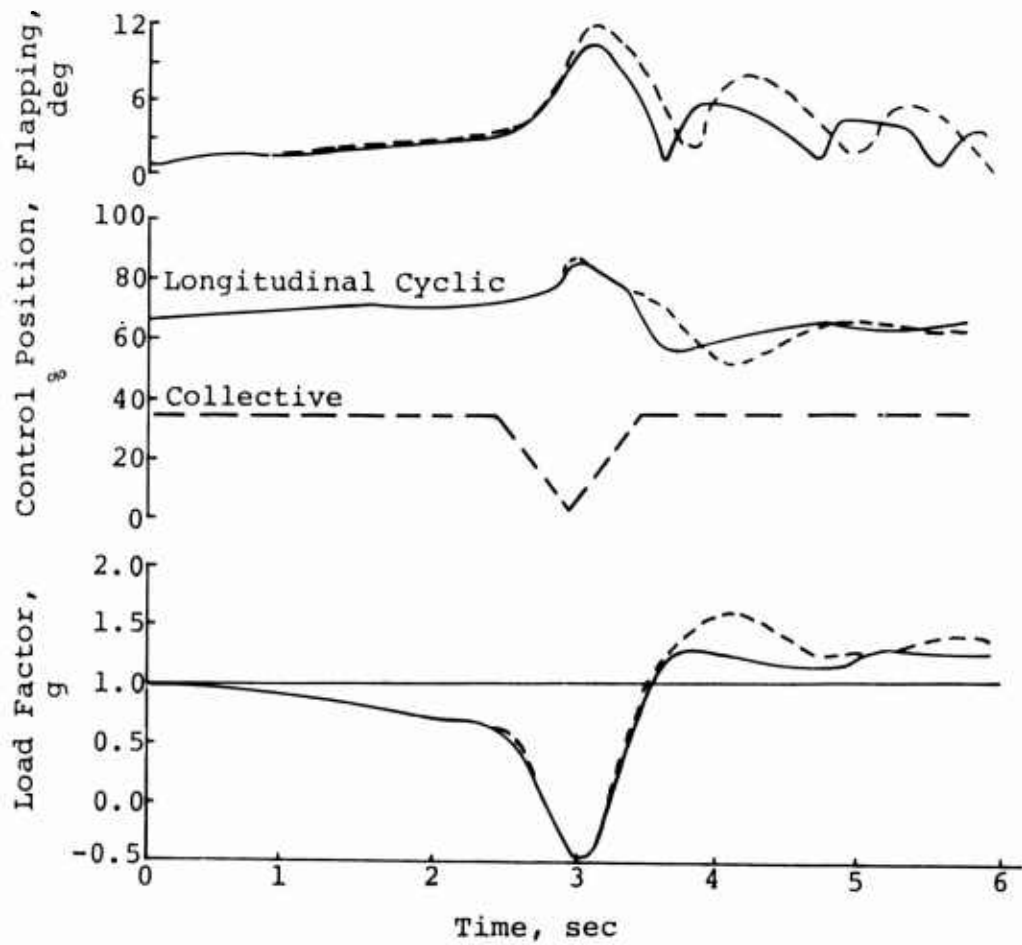


Figure 25. The effect of a nonlinear hub spring on flapping in a push-over maneuver.

4.3 STOP CONTACT LOAD ALLEVIATION

If the rotor hub contacts the mast while in flight, the loads in the mast increase significantly. In this section, the load carrying capabilities of the main rotor mast and possible load alleviation devices are discussed.

4.3.1 Thick Wall Mast

To determine the structural capability of the main rotor mast, the applied loads which may occur under design flight conditions must be considered. The principal inflight loads applied to the mast of a teetering rotor helicopter are illustrated in Figure 26.

The mast is structurally analyzed to determine limit and ultimate load capability at any station along the mast for these types of loads (limit load = ultimate load/factor of safety). An example is presented in Figure 27 for the flapping stop waterline on the baseline, or thin wall mast. Also shown is the range of normal operational loads. It is apparent from these data that considerable excess capability for bending moment exists, particularly at low torsional loads, and the critical design load is the applied rotor torque.

When flapping contact is assumed, the applied bending moment will not be just the shear load component of thrust at the teetering pin, but an additional shear couple between the teetering pin and the flapping stop as shown in Figure 28. The shear load at the flapping stop must now be considered with respect to its local effect on the mast. If the portion of the mast in the area of the flapping stop yields due to the flapping stop load, the torque-carrying capability of the mast is reduced. Thus, the bending moment boundary of Figure 29 must be based on the shear couple which produces flapping stop yielding.

As more powerful engines were used in the AH-1 and UH-1 helicopters, additional torsional capability was required for the mast. The mast wall thickness was increased by 37 percent and mast weight by 17 pounds. The thick wall mast was designed to be retrofitable in helicopters equipped with the original mast. The additional torsional load capability increased the bending moment and shear load capability of the mast at the flapping stop location. This increase is illustrated in Figure 30, and the increased safety margin for applied loads is apparent.

In summary, the thick wall mast is helpful toward expanding the mast load capability envelope but more information is required concerning the magnitude and character of the applied loads due to flapping stop contact before the full benefit of the thick wall mast is assessable.

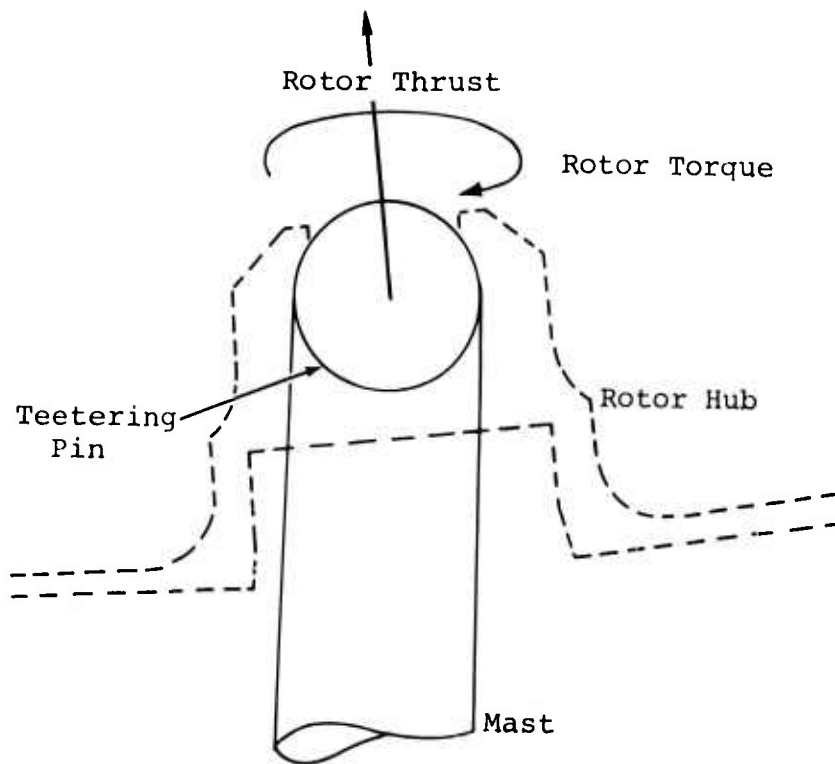


Figure 26. Design flight loads for a teetering rotor helicopter.

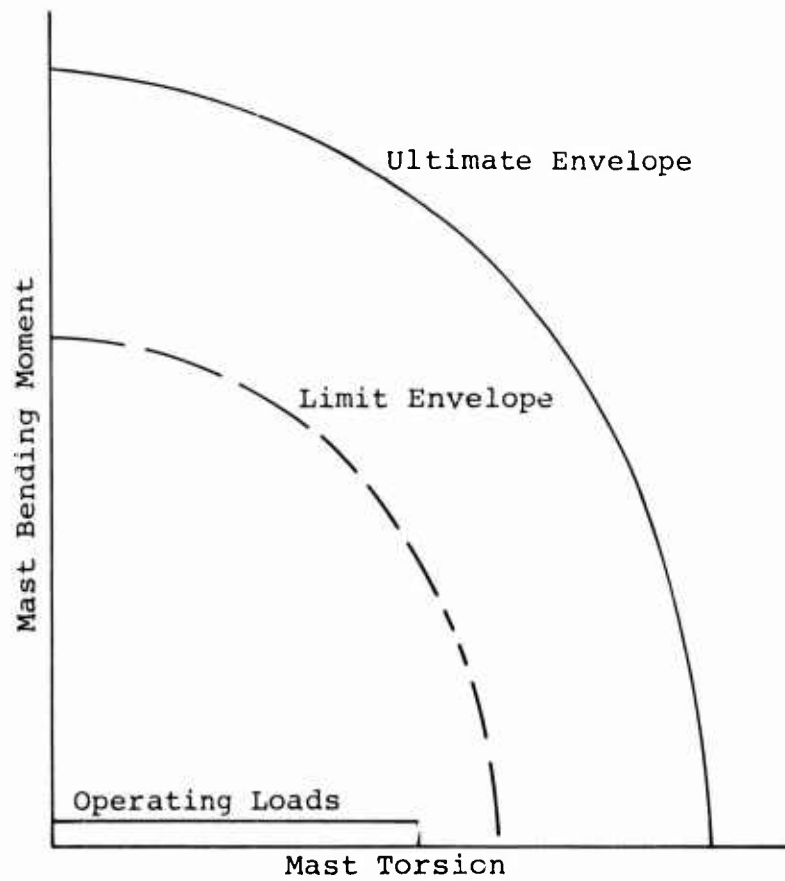


Figure 27. Mast load capabilities at the flapping stop waterline.

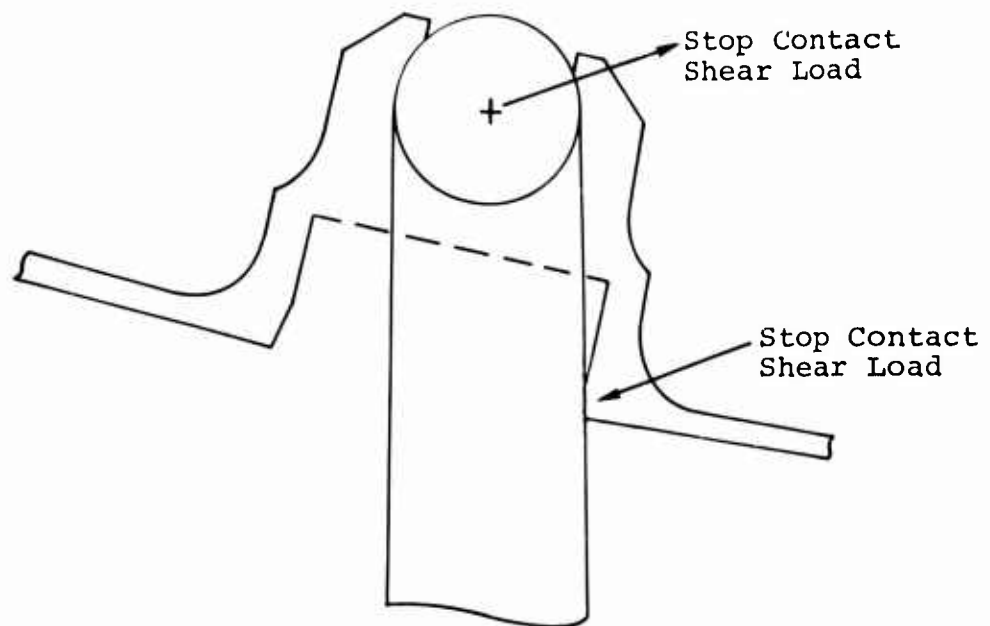


Figure 28. Shear loading due to flapping stop contact.

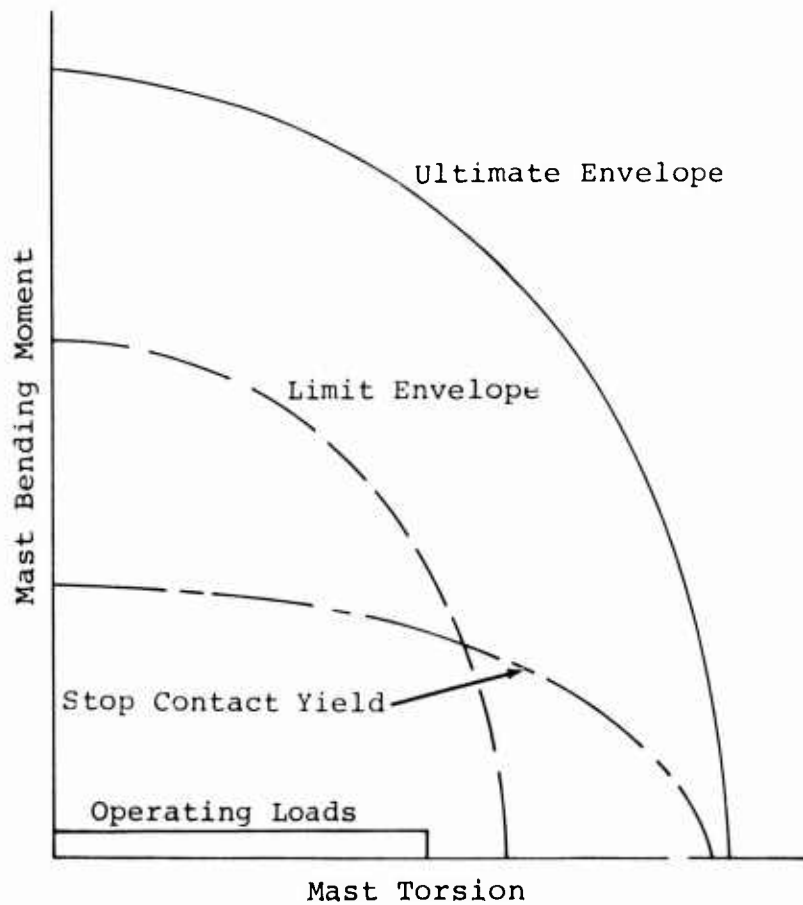


Figure 29. Mast load capabilities at the flapping stop waterline with stop contact.

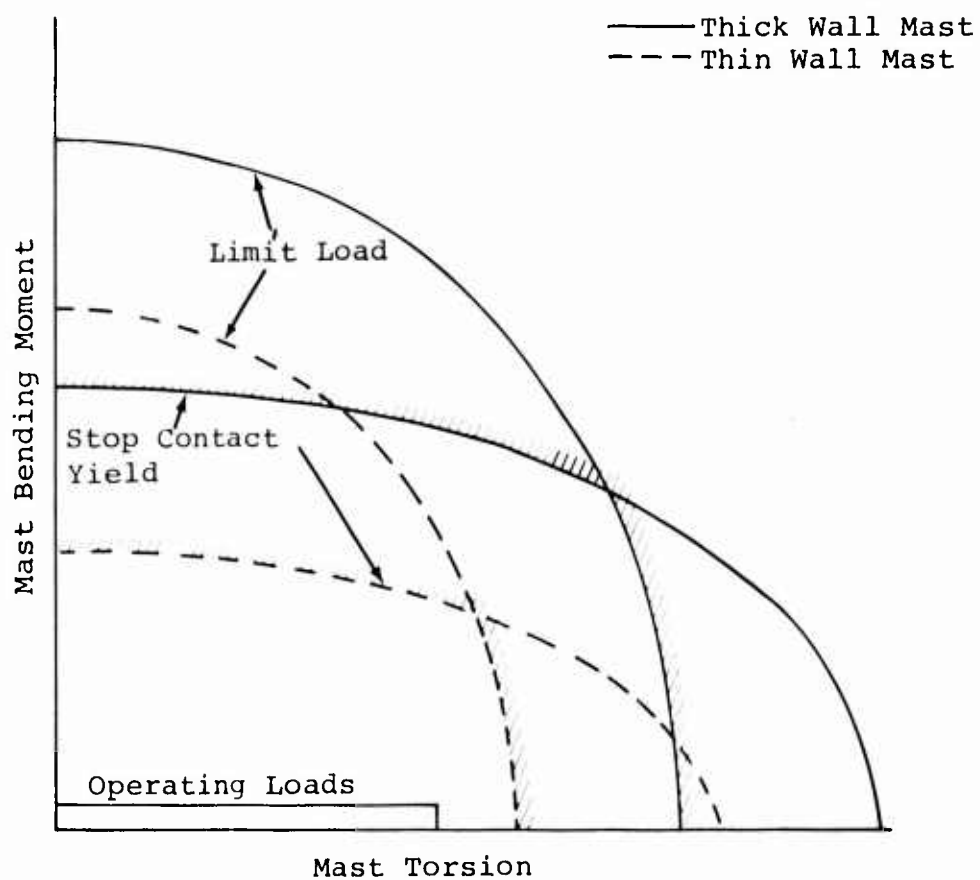
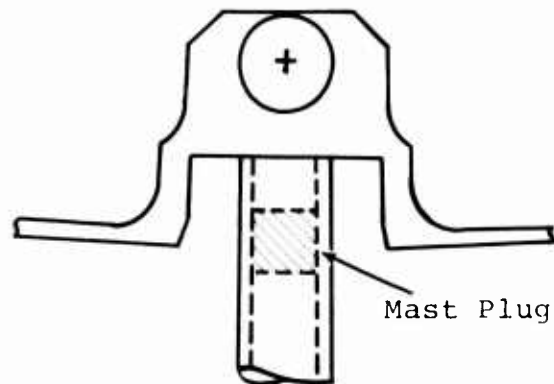


Figure 30. Effect of thick wall mast on mast load capabilities at the flapping stop waterline.

4.3.2 Mast Plug

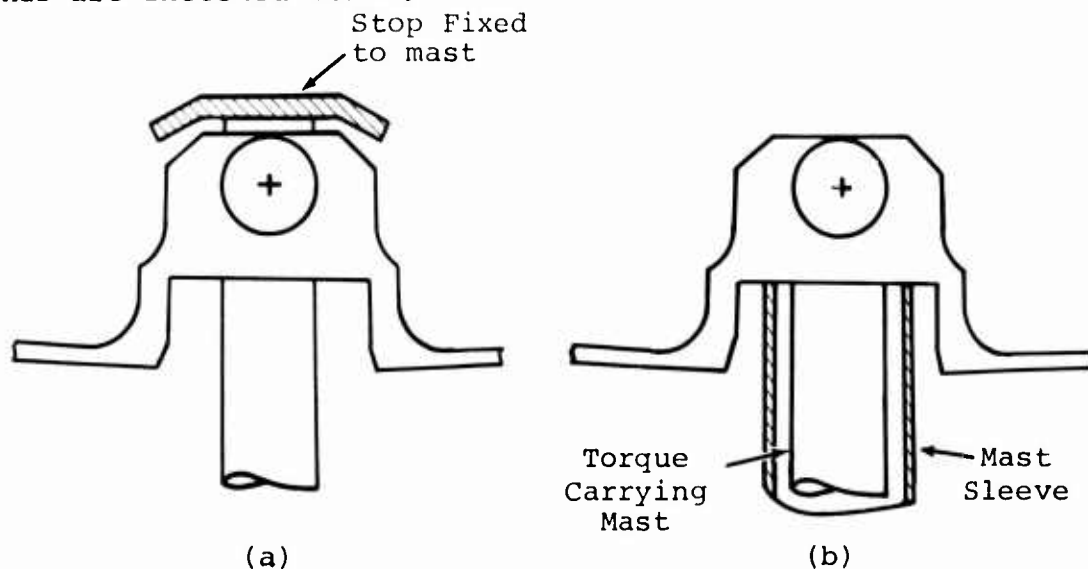
An alternate method of increasing the flapping stop load-carrying capability of the mast is to insert a "plug" inside the main rotor mast at the flapping stop location as shown below:



While providing increased stop contact yield strength, no additional torque carrying capacity is achieved with this plug. This factor, plus possible corrosion and fretting, tends to reduce the desirability of this method to alleviate stop contact loads.

4.3.3 Alternate Stop Locations

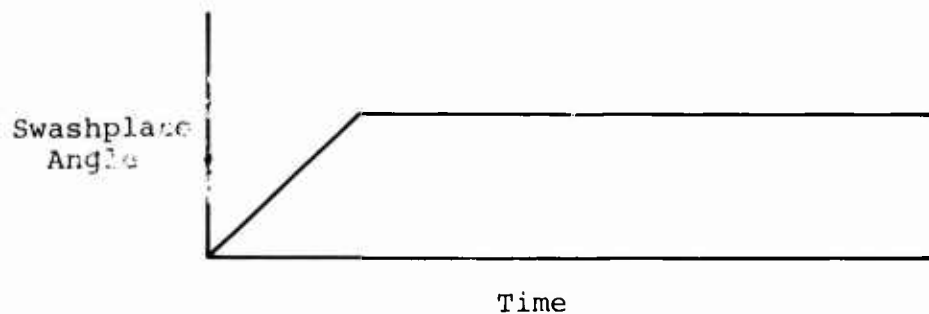
The loss of torque capability due to flapping-stop yielding may be avoided by locating the stop in the structure that carries no drive torque. Two possible methods of achieving this are sketched below.



In both cases, some yielding of the flapping stop would not affect the torque-carrying capability of the rotor mast. For method (a), the limit of allowable stop yielding would be that amount required to allow hub contact with another surface. With method (b), the limit would be the deformation required to cause the sleeve to contact the driving mast.

4.3.4 Energy Absorption Methods

To obtain some knowledge of the load magnitude in the hub, mast and blade assemblies produced by flapping stop contact, an AH-1 helicopter, configured with elastic blades, was modeled on the digital version of C81. The helicopter and pylon were considered rigid and tied down and the rotor was producing no thrust. This provides a conservative estimate of stop loads for the cases considered because mast flexibility and aircraft motion can reduce loads. Flapping was commanded using longitudinal cyclic control inputs of the form shown in the sketch below:



The inputs varied the initial swashplate angle, the rate of change of swashplate angle, and the final swashplate angle. Results of these simulations indicated that, for the assumptions used here, only the final swashplate angle significantly affected the maximum hub load.

The other variables investigated were the flapping stop stiffness and the flapping stop angular location. The hub load was found to depend primarily on the amount of commanded flapping which exceeded the flapping stop angle (i.e., flapping stop at $\pm 10^\circ$, flapping commanded to $\pm 12^\circ$ thus exceeding the stop angle by 2°) rather than on the angular location of the stop. The magnitude of the hub load was directly related to the stop stiffness, with higher loads for higher stiffnesses. As expected, the peak hub loads occurred when the blades were very close (within $\pm 10^\circ$) to the longitudinal axis of the helicopter. Depending on stop location, swashplate rate, and the

maximum swashplate position, the peak loads occurred within 1 to 3 rotor revolutions after the maximum swashplate angle was reached.

The hub loads predicted by C81 for a given increase in a flapping level is less than the increase predicted by straight application of the stop spring rate. This decrease is partially due to the lower flapping caused by the spring and partially due to the blade bending relief.

For the conditions considered here, the use of predicted flapping beyond the stop multiplied by the stop spring rate should provide a conservative estimate of hub load for design. A reduction in flapping stop spring rate could be accomplished through a more flexible mast or, more easily, by imposing a spring rate of the stop through the familiar springs-in-series equation

$$\frac{1}{K_{\text{eff}}} = \frac{1}{K_{\text{stop}}} + \frac{1}{K_{\text{add}}}$$

or

$$\frac{K_{\text{stop}}}{K_{\text{eff}}} = 1 + \frac{K_{\text{stop}}}{K_{\text{add}}}$$

If $K_{\text{add}} = K_{\text{stop}}$, the effective spring rate could be reduced by one-half and the hub loads reduced accordingly.

Several methods are available for supplying this additional spring. Reduced mast stiffness is a possibility, although the effect on mast strength would, of course, be of critical interest. It may also be possible to alter pylon spring rates or geometry to reduce stiffness, but again many factors such as vibration, trim capability at cg extremes, and engine alignment problems must be considered.

A hub spring, similar to the one described in Section 4.2.4, can also be used to introduce stiffness in series with the stop. The nonlinear spring could be tailored to provide the required stiffness to reduce the loads at stop contact.

A brief examination was made of absorbing the flapping energy before stop contact was made. If viscous dampers were attached to the rotor, the effective rotor damping, which normally comes entirely from rotor aerodynamics, can be increased. However, the normal aerodynamic damping is so large that large viscous dampers must be provided to increase this damping significantly. The detrimental effects of large viscous dampers are felt to outweigh the advantages. The forces that must be produced by the dampers would be largest at 90 degrees to peak flapping.

Since flapping is in the direction we wish to produce moments, the dampers would provide moments at 90 degrees to the desired direction. This cross coupling would be undesirable.

4.4 RESULTS OF METHODS STUDY

The three categories of methods to extend the operational envelopes of the helicopter all either reduced the likelihood of inflight flapping stop contact or reduced the consequences of stop contact. The most promising method studied is the use of hub restraint. This was the only method that provided roll control power at low g-levels in addition to reducing flapping in steady flight and maneuvers.

The first category considered was to allow more flapping before contacting the stops. This would give greater inflight stop contact margins but would increase the likelihood of rotor/fuselage strikes.

The methods to control flapping with the use of flight controls would restrict the pilot's ability to generate high flapping control commands. However, the design requirements of acceptable handling qualities and of controlling flapping in conditions of severe blade stall or low-g conditions make these methods less attractive.

Methods to alleviate the loads due to inflight flapping stop contact are desirable and effective. However, loads due to stop contact are not fully understood and more work is necessary to provide design guidelines for structural design. These methods, however, do not prevent high flapping.

The nonlinear hub restraint proposed provides both decreased flapping in all flight conditions and, through the additional control power and damping, enhances the aircraft handling qualities. With the bumper design, the loads due to inflight flapping stop contact are distributed, thus reducing the likelihood of stop yielding.

5. CONCLUSIONS AND RECOMMENDATIONS

5.1 CONCLUSIONS

Flapping in severe maneuvers can be satisfactorily predicted using the hybrid version of the Rotorcraft Simulation Program C81. Matching of flight test data is possible with little modification to original control inputs. Prediction of flapping in future maneuvers is dependent on the interpretation of the computer operator on how a pilot would move the controls during the maneuver.

The most critical operational envelope with regard to rotor blade flapping limits for the AH-1 helicopter, based on the simulation performed in this study, is the low-g flight restriction. Longitudinal center-of-gravity location was also important, but the other envelopes appeared to have only minor effects on flapping. Pilot technique was found to have a significant effect on flapping in maneuvers. The use of large, abrupt control inputs increased flapping over what was seen with more gradual inputs.

The most promising method of alleviating the loads due to high flapping is incorporation of a hub flapping restraint mechanism. This mast moment spring provides additional control power in low-g flight and, in general, reduces flapping in most other flight conditions. Other possible methods involve control system modifications that restrict or correct pilot inputs that may generate high flapping.

5.2 RECOMMENDATIONS FOR FURTHER STUDY

A nonlinear hub spring should be flight tested for a practical feasibility study. While analysis allows prediction of the effect of the hub spring on flapping, its impact on other important factors such as rotor system loads, vibration, and handling qualities would best be examined in hardware testing.

More work is needed to accurately evaluate the loads on the mast due to inflight flapping stop contact. This is required to define a design criterion that ensures no failure of primary structure due to inflight stop contact.

The operational use of the helicopter dictates, to some extent, the maneuvers that must be performed. Investigation of current and projected Army tactics is necessary to assess high flapping situations that may occur. Recommendations for revised procedures can then be made to avoid flapping problems.

The influence of elastic rotor effects on flapping maneuvers also needs to be more fully determined. The severity of the maneuvers required to generate high flapping is such that aeroelastic effects may significantly affect the hub flapping prediction.

REFERENCES

1. Dooley, L. W., ROTOR BLADE FLAPPING CRITERIA INVESTIGATION, USAAMRDL Technical Report 76-33, Eustis Directorate, U. S. Army Air Mobility Research and Development Laboratory, Fort Eustis, Virginia, December 1976, AD A034459.
2. Davis, J. M., et al., ROTORCRAFT FLIGHT SIMULATION WITH AEROELASTIC ROTOR AND IMPROVED AERODYNAMIC REPRESENTATION, USAAMRDL Technical Report 74-10A, B, C, Eustis Directorate, U. S. Army Air Mobility Research and Development Laboratory, Fort Eustis, Virginia, June 1974, AD 782854, 782756, 782841.
3. Anon., OPERATOR'S MANUAL, ARMY MODEL AH-1G HELICOPTER, TM 55-1520-221-10, Headquarters, Department of the Army, May 1975.
4. Magnuson, R. A., STRUCTURAL DEMONSTRATION RESULTS FOR THE IRANIAN MODEL 214A HELICOPTER, Bell Report 214-099-079, Bell Helicopter Textron, Fort Worth, Texas, April 1975.
5. Blaha, J. T., HANDLING QUALITIES DEMONSTRATION OF THE IRANIAN MODEL 214A HELICOPTER, Bell Report 214-099-079, Bell Helicopter Textron, Fort Worth, Texas, February, 1975.
6. Dooley, L. W., COMPARISON OF HYBRID C81 SIMULATION TO FLIGHT TEST RESULTS FOR MANEUVERS CAUSING LARGE FLAPPING, Bell Report 699-099-032, Bell Helicopter Textron, Fort Worth, Texas, October 1976.
7. Blaha, J. T., STRUCTURAL DEMONSTRATION RESULTS FOR THE ICAM PROGRAM, Bell Report 209-099-415, Bell Helicopter Textron, Fort Worth, Texas, May 1975.
8. Melton, J. R., RESULTS OF THE FLIGHT TEST INVESTIGATION OF THE REDUCED G MANEUVER IN THE AH-1G HELICOPTER, Bell Report 209-099-309, Bell Helicopter Textron, Fort Worth, Texas, October 1969.
9. Nicholson, B. M. and Buss, M. W., AH-1G (HUEYCOBRA) HELICOPTER AUTOROTATIONAL ENTRY CHARACTERISTICS, USAASTA Project No. 70-25, U. S. Army Aviation Systems Test Activity, Edwards Air Force Base, California, April 1971.
10. Wells, C. D. and Wood, T. L., MANEUVERABILITY - THEORY AND APPLICATION, JOURNAL OF THE AMERICAN HELICOPTER SOCIETY, Vol. 18, No. 1, January 1973.

LIST OF SYMBOLS

b	number of blades
c	chord of blades, ft
K_1, K_2	transfer function gains
K_{add}	spring rate of additional spring, ft-lb/deg
K_{stop}	flapping stop spring rate, ft-lb/deg
K_{eff}	effective spring rate, ft-lb/deg
R	rotor radius, ft
t_c	blade loading coefficient = thrust/ $\frac{1}{2} \rho (\Omega R)^2 b c R$
x	control displacement, in.
\dot{x}	rate of control displacement, in./sec
ρ	air density, slugs/ft ³
Ω	rotor rotational speed, rad/sec